PHYSICAL REVIEW D **72,** 114510 (2005)

Two flavor QCD and confinement

Massimo D'Elia*
Dipartimento di Fisica dell'Università di Genova, Italy and INFN, Sezione di Genova, Via Dodecaneso 33, I-16146 Genova, Italy

Adriano Di Giacomo† and Claudio Pica‡
Dipartimento di Fisica dell'Università di Pisa, Italy and INFN, Sezione di Pisa, largo Pontecorvo 3, I-56127 Pisa, Italy
(Received 25 March 2005; revised manuscript received 10 November 2005; published 20 December 2005)

We argue that the order of the chiral transition for $N_f = 2$ is a sensitive probe of the QCD vacuum, in particular, of the mechanism of color confinement. A strategy is developed to investigate the order of the transition by use of finite size scaling analysis. An in-depth numerical investigation is performed with staggered fermions on lattices with $L_t = 4$ and $L_s = 12$, 16, 20, 24, 32 and quark masses am_q ranging from 0.01335 to 0.307036. The specific heat and a number of susceptibilities are measured and compared with the expectations of an $O(4)$ second order and of a first order phase transition. A detailed comparison with previous works, which all use similar techniques as ours, is performed. A second order transition in the $O(4)$ and $O(2)$ universality classes are incompatible with our data, which seem to prefer a first order transition. However we have $L_t = 4$ and unimproved action, so that a check with improved techniques (algorithm and action) and possibly larger L_t will be needed to assess this issue on a firm basis.

DOI: 10.1103/PhysRevD.72.114510 PACS numbers: 12.38.Gc, 05.70.−a, 11.30.Rd

I. INTRODUCTION

$N_f = 2$ QCD can provide fundamental insight into the mechanism of confinement. A schematic view of the phase diagram is shown in Fig. 1 [1]. The quark masses are assumed to be equal for the sake of simplicity: $m_u = m_d = m$; μ is the baryon chemical potential.

Consider the plane $\mu = 0$. As $m \to \infty$ quarks decouple and the system tends to the quenched limit. There the deconfining transition is well understood: the transition is an order-disorder first order phase transition, the symmetry involved is Z_3, and the Polyakov line $\langle L \rangle$ is an order parameter. In the presence of quarks Z_3 is explicitly broken and $\langle L \rangle$ is not a good order parameter. Empirically, however, it works as an order parameter at quarks masses down to $m \simeq 2.5$-3 GeV.

At $m \simeq 0$ a chiral phase transition takes place at $T_c \simeq 170$ MeV, from the low temperature phase where chiral symmetry is spontaneously broken to a phase in which it is restored: the chiral condensate $\langle \bar{\psi}\psi \rangle$ is the corresponding order parameter. At some temperature $T_A \geq T_c$ also the $U_A(1)$ symmetry, which is broken by the anomaly, is expected to be effectively restored.

It is not understood what the chiral transition has to do with the deconfining transition, but empirically the Polyakov line has a rapid increase at the transition temperature, indicating deconfinement.

More generally the transition line in Fig. 1 is defined by the maxima of a number of susceptibilities (C_V, χ_m, ...) which all coincide within errors, and which indicate a rapid variation of the corresponding parameters across the line.

A renormalization group analysis plus ϵ-expansion techniques can be made at $m \simeq 0$, assuming that the relevant degrees of freedom for the chiral transition are scalar and pseudoscalar fields [2–4], or more precisely that the order parameters are the vacuum expectation values (v.e.v.) of the following fields

$$\tilde{\phi}\text{: } \phi_{ij} \equiv \langle \bar{q}_i (1 + \gamma_5) q_j \rangle \quad (i, j = 1, \ldots, N_f). \tag{1}$$

Under chiral and $U_A(1)$ transformations of the group $U_A(1) \otimes SU(N_f) \otimes SU(N_f)$, $\tilde{\phi}$ transforms as

$$\tilde{\phi} \to e^{i\alpha} U_+ \tilde{\phi} U_- \tag{2}$$

so that by the usual symmetry arguments, and neglecting irrelevant terms

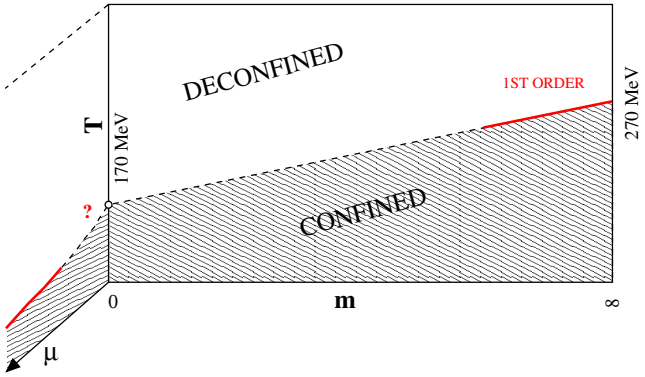

FIG. 1 (color online). Schematic phase diagram of $N_f = 2$ QCD.

*Electronic address: delia@ge.infn.it
†Electronic address: digiaco@df.unipi.it
‡Electronic address: pica@df.unipi.it

$$\mathcal{L}_\phi = \frac{1}{2}\mathrm{Tr}\{\partial_\mu \phi^\dagger \partial^\mu \phi\} - \frac{m_\phi^2}{2}\mathrm{Tr}\{\phi^\dagger\phi\} - \frac{\pi^2}{3}g_1(\mathrm{Tr}\{\phi^\dagger\phi\})^2 - \frac{\pi^2}{3}g_2\mathrm{Tr}\{(\phi^\dagger\phi)^2\} + c[\det\phi + \det\phi^\dagger]. \quad (3)$$

The last term describes the anomaly: indeed it is $SU(N_f) \otimes SU(N_f)$ invariant, but not $U_A(1)$ invariant.

A second order phase transition corresponds to an infrared (IR) stable fixed point. For $N_f \geq 3$ the effective action is of the form Eq. (3) and no such point exists so that the transition is first order. For $N_f = 2$, $\det\phi$ has mass dimension 2 so that other relevant terms emerge, like $(\det\phi + \det\phi^\dagger)^2$ and $Tr\{\phi^\dagger\phi\}(\det\phi + \det\phi^\dagger)$. If the anomaly term in Eq. (3) vanishes ($c \simeq 0$), i.e. if the η' mass vanishes at T_c, then there is no IR stable fixed point and the transition is first order. If instead $c \neq 0$ the symmetry is $SU(2) \otimes SU(2) \simeq O(4)$ and a fixed point exists which can produce a second order phase transition.

In the first case the phase transition is first order also at $m \neq 0$ and most likely up to $m = \infty$.

In the second case a phase transition is only present at $m = 0$, which goes into a continuous crossover as $m \neq 0$: this is true also in the presence of a small chemical potential $\mu \neq 0$, so that a tricritical point is expected in the T-μ plane (see Fig. 1) at the border of the crossover with the first order transition line which takes place in the small T, large μ region [5]. Proposals exist to detect the tricritical point in heavy ion collisions: obviously no such point exists if the transition at $\mu = 0$ is first order.

The issue is in fact fundamental. If confinement is an absolute property of the QCD vacuum and the deconfinement transition corresponds to a change of symmetry (order-disorder), then a crossover is excluded and the only allowed possibility is that the transition is always first order. The argument also extends to the case of $2 + 1$ flavors, of which Fig. 1 is a boundary [6]. The question deserves a careful study.

A few groups have investigated the problem on the lattice with staggered [6–12] or Wilson [13] fermions. The strategy used has either been to look for signs of discontinuity at the transition, or to study the dependence on m of the peak of different susceptibilities, or to study the magnetic equation of state. No clear sign of discontinuity has been observed, but also no conclusive agreement of scaling with $O(4)$ critical indexes. In particular the thermal exponent $y_t = 1/\nu$ (see Section II for the definition) determined using staggered fermions differs significantly from that of $O(4)$-$O(2)$ (no direct determination of the critical exponents exists for Wilson quarks). A general tendency exists however in the community to consider the chiral transition second order, and the line of Fig. 1 a crossover.

In the present work we have made a big numerical effort and used large lattices attempting to clarify the issue. Like most of the other works we use nonimproved Kogut-Susskind action, and lattices $4 \times L_s^3$ with $L_s = 12$, 16, 20, 24, 32. Some scaling violations are expected and a more careful study with $L_t = 6$ and an improved action is planned in order to control them.

A preliminary account has been presented at conferences [14]. The present paper contains more data and a full analysis.

The paper is organized as follows: In Section II we explain the strategy used to attack the problem. Section III contains details about the simulations and the numerical results. Section IV contains the analysis of scaling. Section V contains a discussion and the conclusions.

II. STRATEGY

The theoretical tool to investigate the order of a phase transition is finite size scaling [15,16]. The extrapolation from finite size L_s to the thermodynamical limit $L_s = \infty$ is governed by the critical indexes, which identify the order and the universality class of the transition.

Approaching the transition, for a higher order or weak first order transition, the correlation length of the order parameter ξ goes large compared to the lattice spacing a, so that the dependence of physical quantities on a/ξ can be neglected. More precisely, if $\mathcal{L}/kT$ is the effective action (density of free energy)

$$\frac{\mathcal{L}}{kT} \simeq L_s^{-d}\phi\left(\frac{a}{\xi}, \frac{L_s}{\xi}, am_q L_s^{y_h}\right), \quad (4)$$

the dependence on a/ξ disappears as T_c is approached, since ξ diverges as

$$\xi \simeq_{\tau\to\infty} \tau^{-\nu}, \quad (5)$$

where $\tau \equiv 1 - \frac{T}{T_c}$. The variable L_s/ξ can be traded with $\tau L_s^{1/\nu}$ and the scaling law follows

$$\frac{\mathcal{L}}{kT} \simeq L_s^{-d}\phi(\tau L_s^{1/\nu}, am_q L_s^{y_h}). \quad (6)$$

The problem has two scales, ξ and $1/m_q$. The effective action depends on the order parameter, as dictated by the symmetry, and as $\tau \to 0$ irrelevant terms can be neglected. The thermodynamics is described by correlators of the order parameter, which contain information on the discontinuities of the thermodynamical quantities. The most fundamental quantity is the specific heat, which is always guaranteed to exhibit the correct critical behavior, independently of the identification of the correct order parameter.

For the specific heat the scaling law is

$$C_V - C_0 \simeq L_s^{\alpha/\nu} \phi_c(\tau L_s^{1/\nu}, am_q L_s^{y_h}); \tag{7}$$

C_0 stems from an additive renormalization [16].

For the susceptibility χ of the order parameter $O(x)$

$$\chi = \int d^3x [\langle O(x)O(0)\rangle - \langle O\rangle^2], \tag{8}$$

the scaling law is

$$\chi \simeq L_s^{\gamma/\nu} \phi_\chi(\tau L_s^{1/\nu}, am_q L_s^{y_h}). \tag{9}$$

We shall discuss the question if a subtraction is needed for χ as for the specific heat in Section IV D.

Analogous scaling laws can be derived for mixed susceptibilities.

The values of the indexes characterize the transition: the values relevant to the analysis which follows are listed in Table I. $O(4)$ is the symmetry expected if the chiral transition is second order, but it can break down to $O(2)$ by the lattice discretization for Kogut-Susskind fermions [9] at nonzero lattice spacing.

The scaling law in Eq. (7) for the specific heat is valid independent of the knowledge of the order parameter. The scaling law in Eq. (9) instead is correct only if the choice of the order parameter is the right one. In principle the matching between (7) and (9) can be used to legitimate any guess on the symmetry and on the order parameter.

The scaling laws (7) and (9) are difficult to test because they depend on two variables. A possible strategy is to keep one of them fixed and to study the scaling with respect to the other. As one can see in Table I, the index y_h is the same within errors for $O(4)$ and $O(2)$ symmetry. In order to reduce the problem to one scale, we have made a number of simulations at different values of L_s and am_q keeping $am_q L_s^{y_h}$ fixed and assuming $y_h = 2.49$ which corresponds to $O(4)$ or $O(2)$. In this way as L_s is increased, $am_q \to 0$, so that the infinite volume limit corresponds to the chiral transition at $am_q = 0$.

From Eqs. (7) and (9) it follows that the maxima at constant $am_q L_s^{y_h}$ scale as

$$(C_V - C_0)_{\max} \propto L_s^{\alpha/\nu}, \qquad \chi_{\max} \propto L_s^{\gamma/\nu}, \tag{10}$$

as $L_s \to \infty$ and their positions scale as

$$\tau L_s^{1/\nu} = \text{const.} \tag{11}$$

If $O(4)$ or $O(2)$ is the correct symmetry, the values of ν, α/ν, and γ/ν should be consistent with the corresponding values listed in Table I.

Notice that Eqs. (7) and (9) involve the long range part of the correlations, i.e. they are related to the infrared regime, and are not expected to be significantly affected by scaling violations $O(a/\xi)$.

If the answer to this test is positive the chiral transition is second order at $am_q = 0$ and a crossover at $am_q \neq 0$. If the answer is negative the transition can in principle be of any kind. The analysis of Refs. [2–4], however, suggests to analyze the possibility that the transition is first order, which follows as an alternative if the assumption Eq. (3) about the relevant degrees of freedom is correct. A similar analysis should then be done keeping $am_q L_s^{y_h}$ fixed with $y_h = 3$, the critical index corresponding to first order. In this work we have numerically analyzed the cases of $O(4)$ and $O(2)$. We will analyze the case of first order in a subsequent paper, where we will use an improved action and larger lattices. To test first order vs $O(4)$, $O(2)$ we have used in this work an alternative strategy.

At fixed am_q, β the values of the susceptibility should converge at large L_s if $\mathcal{L}$ is analytic. One can change the variable by replacing $\tau L_s^{1/\nu}$ with the ratio

$$\frac{\tau L_s^{1/\nu}}{(am_q L_s^{y_h})^{1/(\nu y_h)}} = \tau (am_q)^{-1/(\nu y_h)}. \tag{12}$$

The scaling laws Eqs. (7) and (9) become then

$$C_V - C_0 \simeq L_s^{\alpha/\nu} \tilde{\phi}_c(\tau (am_q)^{-1/(\nu y_h)}, am_q L_s^{y_h}), \tag{13}$$

$$\chi \simeq L_s^{\gamma/\nu} \tilde{\phi}_\chi(\tau (am_q)^{-1/(\nu y_h)}, am_q L_s^{y_h}). \tag{14}$$

At large L_s the dependence on $am_q L_s^{y_h}$ must cancel the dependence on L_s in front of the scaling functions in Eqs. (7) and (9). It follows that

$$C_V - C_0 \simeq (am_q)^{-\alpha/(\nu y_h)} f_c(\tau (am_q)^{-1/(\nu y_h)}), \tag{15}$$

$$\chi \simeq (am_q)^{-\gamma/(\nu y_h)} f_\chi(\tau (am_q)^{-1/(\nu y_h)}). \tag{16}$$

The peaks of $(C_V - C_0)$ and of χ should then scale as

$$(C_V - C_0)_{\max} \propto (am_q)^{-\alpha/(\nu y_h)}, \qquad \chi_{\max} \propto (am_q)^{-\gamma/(\nu y_h)}, \tag{17}$$

as $am_q \to 0$. As for the position of the maxima, it scales

TABLE I. Critical exponents.

	y_t	y_h	ν	α	γ	β	δ
$O(4)$	1.336(25)	2.487(3)	0.748(14)	−0.24(6)	1.479(94)	0.3837(69)	4.852(24)
$O(2)$	1.496(20)	2.485(3)	0.668(9)	−0.005(7)	1.317(38)	0.3442(20)	4.826(12)
MF	3/2	9/4	2/3	0	1	1/2	3
1st Order	3	3	1/3	1	1	0	∞

according to

$$\tau(am_q)^{-1/(\nu y_h)} = \text{const.} \tag{18}$$

An alternative possibility is to keep the scaling in the form of Eqs. (7) and (9), and require that the volume dependence disappears at $\tau L_s^{1/\nu}$ fixed. This kind of scaling could work better if the correlation length is comparable to L_s, while $aL_s m_\pi \gg 1$. This implies the scaling laws:

$$C_V - C_0 \simeq (am_q)^{-\alpha/(\nu y_h)} f_c(\tau L_s^{1/\nu}), \tag{19}$$

$$\chi \simeq (am_q)^{-\gamma/(\nu y_h)} f_\chi(\tau L_s^{1/\nu}). \tag{20}$$

Equations (17) for the maxima stay unchanged, but the positions of the maxima scale now as

$$\tau L_s^{1/\nu} = \text{const} \tag{21}$$

and the width of the peaks are volume dependent.

All that is expected to be true at sufficiently large values of $aL_s \cdot m_\pi$ and at sufficiently small values of am_q, such that we are not too far from the critical point. We stress that if there is scaling at all, the validity of Eqs. (15) and (16) or Eqs. (19) and (20) relies on the infrared parameter $aL_s m_\pi$ to be $\gg 1$.

$\tau \equiv 1 - T/T_c$ is usually taken in the literature [9,10] as proportional to $\beta_0 - \beta$, where β_0 is the value of $\beta = 2N_c/g^2$ at the chiral ($am_q = 0$) transition, and all the analyses of the scaling law are based on that choice.

In fact, since

$$T = \frac{1}{L_t a(\beta, am_q)}, \tag{22}$$

the correct definition is

$$\tau \equiv 1 - \frac{T}{T_c} = 1 - \frac{a(\beta_0, 0)}{a(\beta, am_q)} \tag{23}$$

and the dependence on am_q is nontrivial (see e.g. [17]). $a(\beta, am_q)$ is expected to be an analytic function in a neighborhood of the critical point and therefore for sufficiently small $\beta_c - \beta$ and m

$$a(\beta, am_q) \simeq a(\beta_0, 0) + \frac{\partial a}{\partial \beta}(\beta_0, 0)(\beta - \beta_0) + \frac{\partial a}{\partial (am_q)}(\beta_0, 0) am_q. \tag{24}$$

If needed higher orders in am_q and $(\beta - \beta_0)$ can be included. It then follows that at sufficiently small values of am_q

$$\tau = C(\beta_0 - \beta + k_m am_q) \tag{25}$$

with

$$C \equiv \frac{\partial \ln a}{\partial \beta}(\beta_0, 0), \qquad k_m \equiv \frac{1}{C}\frac{\partial \ln a}{\partial am_q}(\beta_0, 0). \tag{26}$$

In the quenched case this reduces to $\tau \propto \beta_0 - \beta$ as usual: in the presence of dynamical quarks $k_m \neq 0$ [17].

The scaling law for the position of the peaks becomes then

$$\beta_0 - \beta_c + k_m am_q = \text{const} \cdot (am_q)^{1/(\nu y_h)}. \tag{27}$$

Equations (15) and (16) should be valid if $L_s \gg \xi/a$, $L_s \gg 1/(am_\pi)$ (see Table II). If the alternative possibility is considered, i.e. requesting that the free energy stays finite when $L_s \to \infty$ at fixed $\tau L_s^{1/\nu}$, the position scales instead as

$$\beta_0 - \beta_c + k_m am_q = \text{const} \cdot L_s^{-1/\nu}. \tag{28}$$

Analogous formulae can be written including quadratic terms of the expansion Eq. (24) (see Section IV below).

An alternative technique is to investigate the order of the transition by looking for discontinuities: if the transition is first order at $m = 0$, it is expected to be so also at $m \neq 0$. If the transition is weak first order, at small volumes compared to some critical volume it will behave as if the free energy were regular, so that Eqs. (15), (16), and (17), or (19) and (20), are expected to be valid, with the critical indexes appropriate to first order. At larger volumes, however, the peak of the specific heat as well as the peaks of the other susceptibilities should increase proportionally to the volume, as a consequence of the discontinuity in the first derivatives of the free energy. At the same time a bistability should appear in the time histories [6]. Such an analysis has been, in particular, performed in Ref. [11,12]: some sign of growth with the volume has been observed, but no significant bistability; we will comment on this result below. Of course if a discontinuity is observed one can conclude that the transition is first order. If not one cannot exclude that it could be observed at larger volumes.

Finally one can investigate the so-called magnetic equation of state [12], i.e. the scaling behavior of the chiral

TABLE II. Run parameters for the numerical simulations.

	Run1				Run2				Other	
L_s	12	16	20	32	12	16	20	32	16	24
am_q	0.153 518	0.075	0.043 03	0.013 35	0.307 036	0.15	0.086 06	0.0267	0.013 35	0.044 44
# Traj.	22 500	87 700	14 520	14 500	25 000	131 390	16 100	15 100	10 000	10 000
$aL_s \cdot m_\pi$	11.9	11.0	10.0	8.9	11.3	15.8	14.8	12.4	4.5	12.2

order parameter itself, $\langle\bar{\psi}\psi\rangle$, versus the reduced temperature. The scaling law is

$$\langle\bar{\psi}\psi\rangle \simeq m^{1/\delta} f(\tau m^{-1/(\nu y_h)}) \tag{29}$$

and again it can provide information on the critical indexes.

III. NUMERICAL SIMULATIONS

A. Algorithm

Monte Carlo simulations were performed using the standard staggered action. The *Hybrid R* algorithm [18] was used for the configuration updating. Since it is a nonexact algorithm, its systematic errors must be kept under control. The finite integration step used in the molecular dynamics evolution introduces a systematic error on the mean values of observables proportional to the integration step squared $\Delta\tau^2$. Great care was taken to ensure that this systematic shift was much smaller than the statistical error in each Monte Carlo run. Typical values of the integration step $\Delta\tau$ vary with the mass of the quarks in units of the lattice spacing as $\Delta\tau = am_q/4$. When the use of that value for the integration step was too prohibitive, i.e. at the smallest quarks masses used in this work, the integration step was in any case taken below $am_q/2$. The stopping condition used for the conjugate gradient inversion was fixed requiring that the residue was smaller than 10^{-8}. The length of the molecular dynamics trajectories was fixed to 1 for all of our simulations.

B. Run parameters

All of our numerical simulations were performed using a lattice temporal extent of $L_t = 4$. To begin with we run two sets of Monte Carlo simulations fixing for each the value of $am_q L_s^{y_h}$ as explained in Section II. The two sets, called in the following Run1 and Run2, have $am_q L_s^{y_h} = 74.7$ and $am_q L_s^{y_h} = 149.4$, respectively. The spatial lattice sizes L_s used for each of the two sets are $L_s = 12, 16, 20, 32$.

Additional simulations at $L_s = 24$ and $am_q = 0.044\,44$ and at $L_s = 16$ and $am_q = 0.013\,35$ were added. The second one was chosen by purpose at the same mass of the $L_s = 32$ of Run1.

A summary of the bare quark masses and L_s used is reported in Table II. The total number of Monte Carlo (MC) trajectories collected is also reported together with the quantity $aL_s \cdot m_\pi$ at the pseudocritical value of the coupling β_c (am_π was taken from the parametrization given by the MILC Collaboration in Ref. [17]). Since for all our runs the spatial extent is much larger than the pion correlation length, no large infrared cutoff effects are expected, except possibly for the run at $L_s = 16$ and $am_q = 0.013\,35$ (see Table II).

For each value of am_q and L_s, MC simulations were performed at different β values in order to inspect and to have under control the whole interesting critical region. See Appendix A, Tables IV, V, and VI, for the whole listing of our run parameters.

C. Data Reweighting

The collected raw data were analyzed using standard statistical procedures (see e.g. [19]). For the history of each observable, thermalizations were taken self consistently to be 5 times the integrated autocorrelation time estimated from thermalized trajectories.

The data collected were analyzed using the multihistogram reweighting technique combining data taken at different β's together. This method allows to extract mean values of observables and their susceptibilities at intermediate β values over the whole range explored with numerical simulations. Using the reweighted data, it is possible to locate accurately the position at which the susceptibilities attain their maximum and their value at the maximum. Sometimes in previous studies a single point with high statistics at about the critical point was used. Using data from simulations done at several β values covering the whole critical region, eliminates the risk of a wrong extrapolation from a single β too distant from the critical point.[1] Moreover the method allows a better sampling of the probability distribution, due to the fact that different simulations are combined together, thus increasing the precision and confidence of the measurement.

The errors of observable quantities were estimated using the bootstrap method. In practice, this means repeating the whole multihistogram reweighting procedure a number of times starting from random data samples distributed as the measured empirical distributions.

D. Observables

For each generated configuration of our MC simulations we measured the average spatial and temporal plaquettes (P_σ, P_τ), the chiral condensate ($\bar{\psi}\psi$), the energy density ($\bar{\psi}D_0\psi$), and the following lattice susceptibilities (the notation is the same as in [11]):

$$\chi_m^{\text{disc}} = \left(\frac{N_f}{4}\right)^2 \frac{1}{V}[\langle(\text{Tr}D^{-1})^2\rangle - \langle\text{Tr}D^{-1}\rangle^2], \tag{30}$$

$$\chi_m^{\text{conn}} = -\frac{N_f}{4V}\sum_{x,y}\langle D_{x,y}^{-1} D_{y,x}^{-1}\rangle, \tag{31}$$

$$\chi_{e,ij} = V[\langle P_i P_j\rangle - \langle P_i\rangle\langle P_j\rangle], \quad i,j = \sigma,\tau, \tag{32}$$

$$\chi_{e,f} = V[\langle(\bar{\psi}D_0\psi)^2\rangle - \langle\bar{\psi}D_0\psi\rangle^2], \tag{33}$$

[1] Remember that for single histogram reweighting the statistics needed in order to extrapolate measured quantities at a value of $\beta = \beta_0 + \Delta\beta$ different from that used in the actual simulation grow exponentially with $\Delta\beta$.

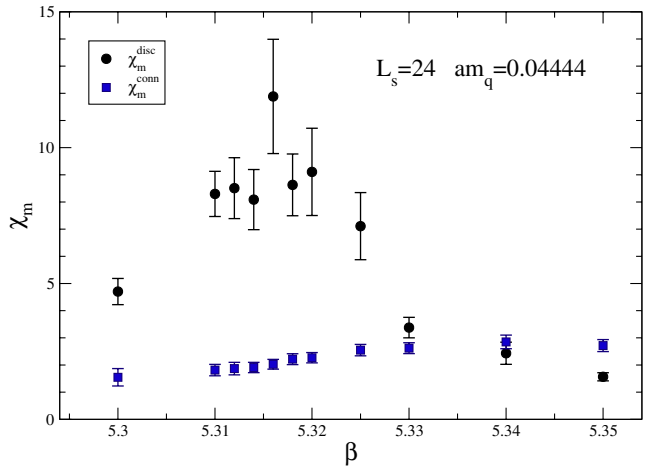

FIG. 2 (color online). Comparison between the connected and disconnected component of χ_m. The former is typically a small fraction of the connected component at the peak position.

$$\chi_{e,i} = V[\langle P_i(\bar{\psi}D_0\psi)\rangle - \langle P_i\rangle\langle\bar{\psi}D_0\psi\rangle], \quad i = \sigma, \tau, \tag{34}$$

$$\chi_{t,i} = V[\langle P_i(\bar{\psi}\psi)\rangle - \langle P_i\rangle\langle\bar{\psi}\psi\rangle], \quad i = \sigma, \tau, \tag{35}$$

$$\chi_{t,f} = V[\langle(\bar{\psi}\psi)(\bar{\psi}D_0\psi)\rangle - \langle(\bar{\psi}\psi)\rangle\langle\bar{\psi}D_0\psi\rangle], \tag{36}$$

where $V = L_s^3 L_t$ is the volume; D_0 is the temporal component of the Dirac operator D.

The connected component of the chiral susceptibility $\chi_m^{\rm conn}$ has not been measured for all of our simulations but only for a fraction of them (see Table VII). The method used to extract $\chi_m^{\rm conn}$ is the volume source method without gauge fixing as described in Ref. [11]. The disconnected component gives the dominant contribution for large volumes and small masses. The connected part is instead relevant at small volumes and relatively large masses. For most of our lattices we have determined the connected part only around the peak, and we have considered it as a constant with respect to β. We estimate that this is a good approximation within our errors. A representative example[2] is shown in Fig. 2 (taken at $L_s = 24$, $am_q = 0.044\,44$). The typical contribution to χ_m of $\chi_m^{\rm conn}$ is less than about 15% of $\chi_m^{\rm disc}$ at the peak value and is a slowly varying function of β.

A comprehensive list of measured values of $\langle P_\sigma\rangle$, $\langle P_\tau\rangle$, $\langle\bar{\psi}\psi\rangle$, $\langle\bar{\psi}D_0\psi\rangle$, and the lattice susceptibilities for our MC simulation can be found in Appendix A (see Tables IV, V, and VI).

IV. SCALING ANALYSIS

The basic thermodynamic susceptibilities, i.e. the specific heat C_V, the chiral susceptibility χ_m, and the mixed susceptibility χ_t

$$C_V = \frac{1}{VT^2}\frac{\partial^2}{\partial(1/T)^2}\ln Z, \tag{37}$$

$$\chi_m = \frac{T}{V}\frac{\partial^2}{\partial m_q^2}\ln Z, \tag{38}$$

$$\chi_t = \frac{T}{V}\frac{\partial^2}{\partial(1/T)\partial m_q}\ln Z \tag{39}$$

can be expressed as sums of the lattice susceptibilities (30)–(36) multiplied by regular functions of β and am_q. Specifically the specific heat C_V is a function of $\chi_{e,ij}$, $\chi_{e,i}$, and $\chi_{e,f}$; χ_t is a function of $\chi_{t,i}$ and $\chi_{t,f}$. The contribution of other susceptibilities entering in the expression of C_V and χ_t involving the quark mass are expected to be negligible in the chiral limit [20]. As for χ_m, $\partial/\partial(m_q)$ in Eq. (38) is intended at constant temperature. Since temperature depends not only on β but also on am_q, the physical χ_m is a combination of $\chi_m^{\rm disc}$, $\chi_m^{\rm conn}$, $\chi_{t,\tau}$, and $\chi_{e,\tau\tau}$ with computable coefficients.

By C_V in the following we mean $\chi_{e,\sigma\sigma}$; the analysis with $\chi_{e,i}$ and $\chi_{e,f}$ is similar and compatible with respect to scaling.

We are interested in studying the singular behavior of C_V, χ_m, and χ_t as the critical surface is approached which is given by the most singular divergent quantity among the lattice susceptibilities corresponding to a given thermodynamical susceptibility.

A. Pseudocritical coupling

One of the observables analyzed in the literature to understand the order of the transition has been the position of the peaks of thermodynamic susceptibilities as a function of am_q. The position of all these peaks happen to coincide at given am_q and L_s, thus defining a unique (pseudo)critical coupling $\beta_c(am_q)$. Previous works in the literature assume $\tau \propto \beta_0 - \beta$, a choice usually based on a strict analogy between QCD and the $O(4)$ statistical model. In fact the correct thermodynamical reduced temperature is given by Eq. (23). In principle the dependence of $a(\beta, am_q)$ on am_q could be measured by use of independent quantities (see e.g. [17]). We will try a fit of the position of β_c by a form like Eq. (27) or (28), which is expected to be valid at sufficiently small values of am_q. To extend the range of validity of the approximation the quadratic terms proportional to am_q^2, $am_q(\beta_0 - \beta)$, and $(\beta_0 - \beta)^2$ may be added:

$$\tau \propto (\beta_0 - \beta) + k_m am_q + k_{m^2}(am_q)^2 + k_{m\beta} am_q(\beta_0 - \beta). \tag{40}$$

A term $k_{\beta^2}(\beta_0 - \beta)^2$ turns out to be negligible. In fact one can write the lattice spacing a as:

[2]For this lattice $\chi_m^{\rm conn}$ was measured for all points.

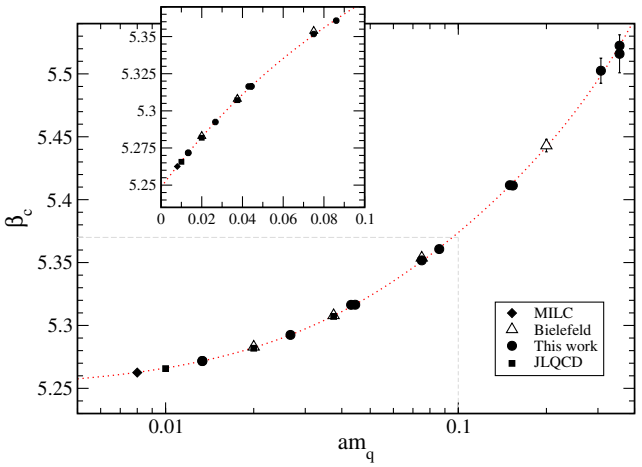

FIG. 3 (color online). (Pseudo)critical couplings determined in this work are shown together with other determinations from the literature. Logarithmic scale is used for the horizontal scale in the main figure, while a linear scale is used for the smaller inset figure. The dotted line is the best fit (χ^2/d.o.f. = 0.89, d.o.f. = 15) curve including am_q^2 and $am_q(\beta_0 - \beta_c)$ terms for masses $am_q < 0.4$.

$$a = \frac{1}{\Lambda(\beta, am_q)}\left(\frac{\beta}{4N_c b_0}\right)^{b_1/2b_0^2} \exp\left(-\frac{\beta}{4N_c b_0}\right), \qquad (41)$$

where the deviation from asymptotic scaling are represented by the fact that the term $\Lambda(\beta, am_q)$ is β dependent. This term is slowly varying with β and can be well described by a linear function of β with coefficients depending on am_q in the relevant range of β's. The k_{β^2} coefficient is given by $\partial^2 \ln a/\partial\beta^2|_{\beta=\beta_0, am_q=0}$ can be computed and can be neglected within errors. The other unknown parameters can be fitted to the data.

Figure 3 shows the critical line $\beta_c(am_q)$. Our determinations (see Table VIII) are reported together with a collection of world data.[3] A good agreement among different determinations can be appreciated.

The expected variation of τ as a function of am_q or L_s is given by Eq. (18) or (21):

$$\tau = k_\tau (am_q)^{1/\nu y_h} \qquad (42)$$

or

$$\tau = k'_\tau L_s^{1/\nu}. \qquad (43)$$

Notice that for a first order transition the exponent of am_q is 1 and the term on the right-hand side of Eq. (42) can be reabsorbed in k_m so that such term can be discriminated only for a second order scaling behavior.

[3]Data of the JLQCD Collaboration are taken from Ref. [11]. We thank E. Laermann and C. DeTar for providing us with the data of the Bielefeld group and of the MILC Collaboration, respectively.

TABLE III. Best fit parameters for the scaling of the pseudocritical coupling. Different kind of fits are explained in the text. k'_τ is set to zero as explained in the text.

β_0	k_m	k_τ	k_{m^2}	$k_{m\beta}$
5.2484(4)	1.84(7)	$\equiv 0$	−0.3(2.4)	−4.3(2.7)
5.2481(13)	1.75(13)	$\equiv 0$	$\equiv 0$	$\equiv 0$
5.2430(40)	1.20(60)	−0.1(1)	−7(6)	6(6)
5.2437(21)	1.12(16)	−0.134(46)	$\equiv 0$	$\equiv 0$

The unknown coefficients k_m, k_{m^2}, $k_{m\beta}$, and k_τ of the expansion of τ around the critical point are determined by use of a best fit procedure. We start from the form Eq. (43). In agreement with previous works we find that the position of the peaks does not depend on the lattice size [9,11], i.e. that $k'_\tau = 0$ within errors implying that no information can be obtained about the order of the transition (first order or second order $O(4)$ or $O(2)$). The quality of the fit assuming $k'_\tau = 0$ is shown in Fig. 3 and the resulting coefficients are listed in the first line of Table III. These coefficients are obtained by a best fit up to a maximum value of am_q, $(am_q)_{\max}$, which is then extrapolated to zero. They are stable and consistent with a linear fit at low values of am_q (< 0.0267) as shown in the second line of Table III.

The scaling of Eq. (21) or (43) assumes that $aL_s m_\pi \gg 1$ but the correlation length ξ can be comparable with L_s, which is certainly true sufficiently close to the critical point in case of a second order or weak first order chiral transition.

We have then analyzed the scaling of the form Eq. (18) or (42). If the transition is first order the analysis coincides with the analysis done for the scaling Eq. (43) and k_m is in fact $k_m - k_\tau$.

If the transition is $O(4)$ a similar analysis can be performed (similar results hold for $O(2)$ or mean field). The χ^2/d.o.f. is acceptable, the result for the coefficients is shown in the third line of Table III. k_τ is consistent with zero, and the result is therefore compatible with that of the first line. However the fit becomes unstable if we try to extrapolate to low masses keeping only the linear term of Eq. (40) (line 4 of Table III).

The critical coupling β_0 and the coefficient k_m are stable both for first order and $O(4)$ behavior and can thus be confidently estimated. Our final estimates, obtained by a weighted average of linear and quadratic fits, are $\beta_0 = 5.2484(5)$ and $k_m = 1.82(8)$ for a first order transition; $\beta_0 = 5.2435(25)$ and $k_m = 1.13(19)$ for $O(4)$. Other terms cannot be reliably estimated with present data. In particular we are not able to discriminate the contribution of quadratic terms from that coming from k_τ and consequently it is not possible to establish the order of the transition by looking at the (pseudo)critical couplings alone.

The possibility to discriminate between the first order and $O(4)$ behavior from the measurement of β_c is in practice very faint. Figure 4 shows the different predictions

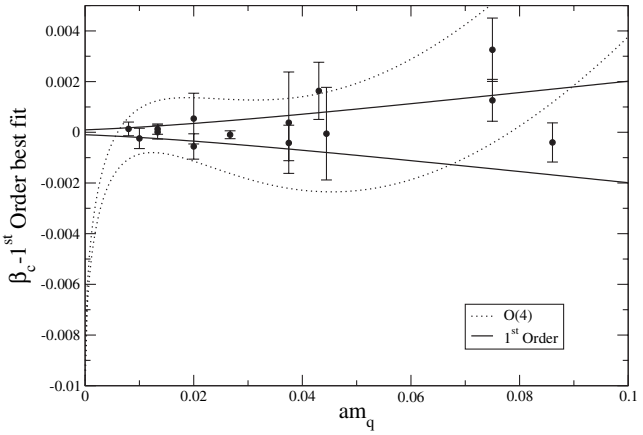

FIG. 4. Different behavior of predicted (pseudo)critical couplings for a first order transition and a second order $O(4)$. Present data do not permit a clear discrimination using only β_c. The 1σ band is displayed. Continuous lines correspond to a first order transition while the dotted lines are the prediction for the $O(4)$ symmetry.

for the (pseudo)critical coupling based on available data. If we discard the high values of the masses a possible difference would only be visible at very small bare quark masses. Using estimates of k_τ shown in Table III a quark mass of about 0.003 should be used, which requires a big numerical effort.

We would like to remark that the explicit dependence of τ on am_q is in any case necessary to fit present data. Fitting to a function of the form

$$\beta_c = \beta_0 + c_\tau (am_q)^{y_t/y_h} \tag{44}$$

with $O(4)$ values for the exponents, gives a $\chi^2/\text{d.o.f.} \simeq 21$ in the interval up to $(am_q)_{\max} = 0.075$, which decreases as $(am_q)_{\max}$ decreases and is ≈ 2 at $(am_q)_{\max} = 0.02$.

As a final remark, the dependence on β and am_q of the lattice spacing a Eq. (23) can be measured from other observables (see e.g. [17]). In particular our estimate for k_m for a first order transition (line 1 of Table III) is compatible with those of Ref. [17] $k_m \approx 1.95$ (affected by errors of order 20%). We notice that $k_\tau = 0$ implies that $\tau = 0$ on the critical line, or, by Eq. (24) that the critical temperature is independent of am_q near the chiral point.

B. Scaling at fixed $am_q L_s^{y_h}$

As explained in detail in Section II, we have adopted a novel strategy in order to simplify the two scales problem. We assume $O(4)$—or $O(2)$—critical behavior and we use this assumption to fix a dependence between am_q and L_s in our Run1 and Run2 so as to fix the second scaling variable in Eq. (6) and reduce the problem to a one scale problem: in this case the only assumption is $O(4)$ itself. This allows us to test whether $O(4)$ is consistent or not with data without any further approximation.

We fixed $am_q L_s^{y_h} = \text{const}$ with $y_h = 2.49$ that is the value expected for $O(4)$ and $O(2)$ critical behavior, with const $= 74.7$ for our Run1 and const $= 149.4$ for Run2. The following scaling formulas should hold (see Eqs. (7) and (9)):

$$C_V(\tau, L_s) - C_0 = L_s^{\alpha/\nu} \Phi_C(\tau L_s^{1/\nu}), \tag{45}$$

$$\chi_m(\tau, L_s) = L_s^{\gamma/\nu} \Phi_\chi(\tau L_s^{1/\nu}), \tag{46}$$

and, in particular, the peaks of the specific heat and χ_m should scale as Eqs. (10).

The subtraction of the noncritical part C_0 for the specific heat is needed. In principle it can be obtained as a parameter from the fit to the maxima of the specific heat. However since we also have data at β's different from the pseudocritical coupling, we were able to perform a direct measurement of this quantity. Appendix B reports the details of the study of the background for C_V. Our final estimate for the background is $C_0(\beta) = 0.400(43) - 0.0663(83)\beta$. Note that the β dependence is very weak and assuming a constant value for the background C_0 does not modify the following analysis. No dependence of C_0 on am_q is observed.

For the susceptibility of the chiral condensate χ_m, for the moment we do not operate any background subtraction.

The measured peak values for the subtracted specific heat $C_V - C_0$ and chiral condensate susceptibility χ_m for Run1 and Run2 are shown in Fig. 5. They are evaluated on the curve obtained by reweighting. The figure shows the peak values of susceptibilities rescaled by the appropriate power of the spatial lattice size Eq. (10). If the scaling laws (10) would hold, the displayed quantity should be a constant. Visibly this is not the case.

The $O(4)$ and $O(2)$ critical behavior is clearly in contradiction with the lattice observation. In particular $O(4)$ and $O(2)$ scaling predicts no singular behavior in the $L_s \to \infty$ limit for the specific heat as the critical exponent α is negative. This means that as L_s is increased, the singular part of C_V should decrease with volume, i.e. that the specific heat should not grow which is in clear contrast with the data. Also for the chiral condensate susceptibility χ_m the predicted exponents fail to reproduce lattice data. In either case the $\chi^2/\text{d.o.f.}$ of the fit with a constant function excludes the behavior of scaling law (10). The full scaling laws Eqs. (7) and (9) were also studied (see Fig. 6). The horizontal scale was obtained by fitting the pseudocritical temperature as described above. As one can expect from the previous discussion, data do not scale according to the predicted laws.

Similar figures are obtained assuming $O(2)$ symmetry.

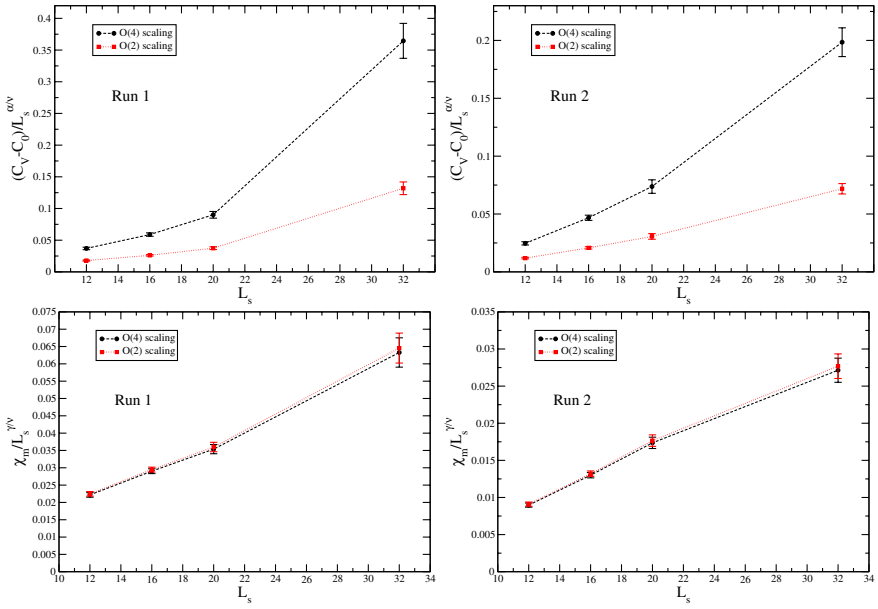

FIG. 5 (color online). Specific heat (top) and χ_m (bottom) peak value for Run1 (left) and for Run2 (right), divided by the appropriate powers of L_s (Eqs. (45) and (46)) to give a constant. Both the $O(4)$ and $O(2)$ critical behaviors are displayed. Notice that for the case of χ_m the ratio γ/ν have almost the same numerical value so that the two curves are almost indistinguishable.

C. Scaling at $L_s \to \infty$

A further scaling test can be done supposing that the lattice size is much larger that all other relevant physical lengths. In such a case one expects that the system shows the same behavior of an infinite system. The scaling laws expected in this case are those of Eqs. (15) and (16). These equations predict no dependence on the parameter L_s. This is the same assumption used in previous scaling analyses of the chiral transition [10–12].

The alternative possibility, illustrated in Section II, is to keep $\tau L_s^{1/\nu}$ (i.e. $\xi/(aL_s)$) fixed thus remaining with the scaling equations Eqs. (19) and (20). Physically this means that the correlation length ξ is not small compared to L_s, which is certainly true in the vicinity of the critical point.

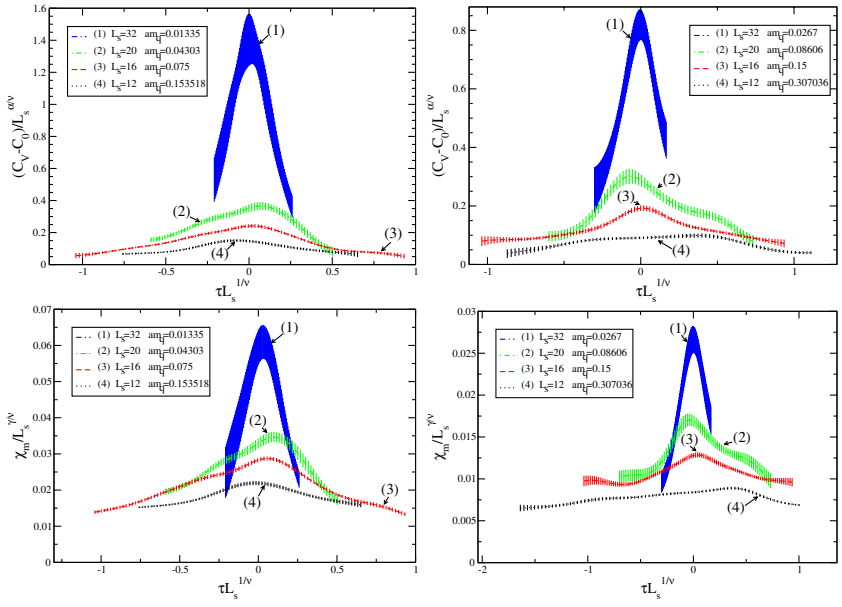

FIG. 6 (color online). Scaling of the specific heat (top) and χ_m (bottom) for Run1 (left) and for Run2 (right), see Eqs. (7) and (9). The curves are obtained by reweighting.

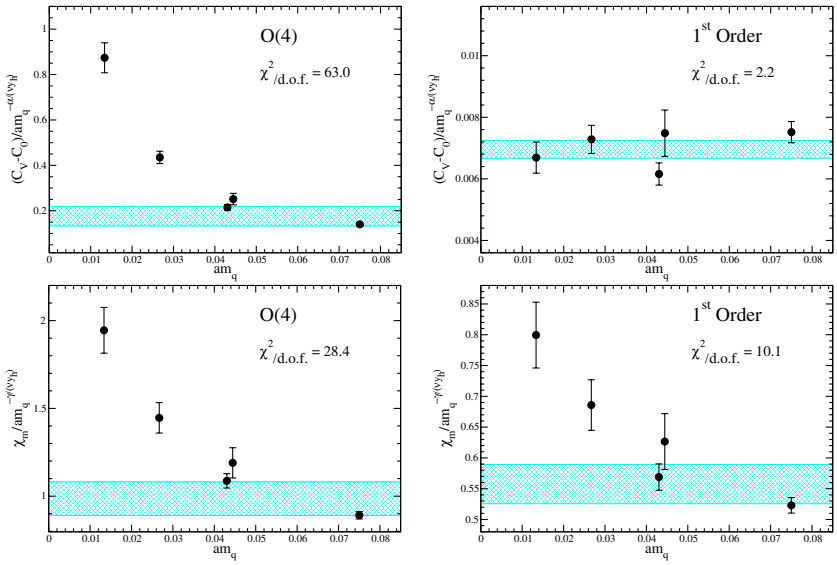

FIG. 7 (color online). Specific heat (top) and χ_m (bottom) peak scaling for $O(4)$ (left) and first order (right).

These scaling laws are only expected to hold for large values of $am_q L_s^{y_h}$ and small masses.

The difference between the two alternatives is only visible by considering the width of the susceptibilities peaks, the heights having the same behavior (see Eqs. (17)).

We have thus first performed the analysis of the scaling of the maxima of the specific heat C_V and χ_m.

We have tested the different critical behaviors compatible with the scenario of Ref. [2], namely $O(4)$, $O(2)$, mean field, and first order. The peak value of the specific heat and of χ_m divided by the appropriate power of the quark mass should be a constant. These ratios are shown in Fig. 7 both for $O(4)$ and first order. The figure shows also the confidence region from a fit with a constant value together with the corresponding χ^2/d.o.f.

From the values of the χ^2/d.o.f. it is easily seen that the second order critical behavior is not compatible with data. It must be noticed that, although the validity region of the scaling law is not known *a priori*, so that the upper mass limit for the fits is somewhat arbitrary, if we further restrict the mass region, the χ^2/d.o.f. for the C_V fits tend to

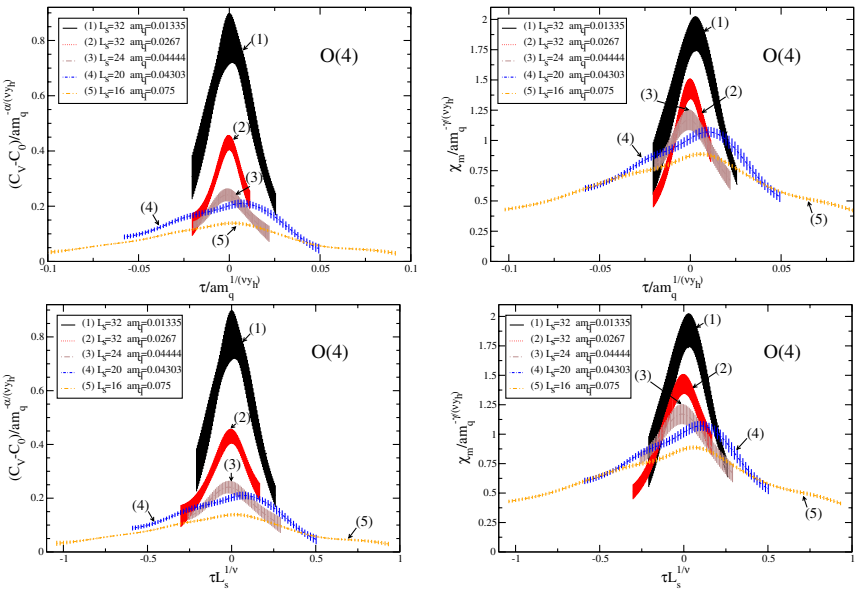

FIG. 8 (color online). Comparison of specific heat (left) and χ_m (right) scaling for $O(4)$. Equation (19), (20) (top) and Eq. (7), (9) (bottom).

increase. We stress that also in previous studies [10–12] the values found for the susceptibility peaks were not compatible with the critical indexes of $O(4)$, $O(2)$, and mean field. On the contrary the first order behavior looks compatible with data (even if the χ^2/d.o.f. is ~ 2) for the specific heat. We will discuss the scaling of χ_m in Section IV D.

The scaling of susceptibilities at all β values can also be investigated. The situation is depicted in Fig. 8 for $O(4)$: all the curves should coincide within errors if there were $O(4)$ scaling. Similar features are observed for $O(2)$ and mean field. No scaling is observed: this is clearly the case for the maxima of the susceptibilities as discussed above, but it is also true for the width of these curves. The analogous figure using first order indexes is shown in Fig. 9. Scaling is observed for the specific heat in the form Eqs. (19) and (20) and not in the form (15) and (16), which does not describe the widths of the peaks. Again for χ_m we postpone the discussion to Section IV D.

Runs with higher values of the masses ($am_q > 0.075$) do not obey the scaling laws. The one with $L_s = 16$ and $am_q = 0.013\,35$, which should coincide with the $L_s = 32$ at the same bare mass, in case of scaling Eqs. (15) and (16) is instead different (see Fig. 10). For scaling Eqs. (19) and (20), the maximum should be the same, and the widths should differ by a factor of 8, and this is not the case. We have carefully checked the stability of the curves obtained by reweighting against variations of the statistics, e.g. by discarding single data points from the analysis. This lack of scaling can be interpreted as due to the small value (4.5) of the parameter $aL_s m_\pi$, invalidating the limit bringing to Eqs. (15), (16), (19), and (20). A similar effect could be responsible for the observed increase of the peak with the volume observed in previous studies [11].

A more careful study of this effect will be done in the future.

D. Magnetic equation of state

As a further test of scaling we check the equation of state Eq. (29). No scaling whatsoever is observed, neither $O(4)$-$O(2)$ nor first order, if the raw measured data are introduced in Eq. (29) (see Fig. 11). Indeed as $\langle\bar{\psi}\psi\rangle$ is different from 0 at large β a subtraction is needed: the

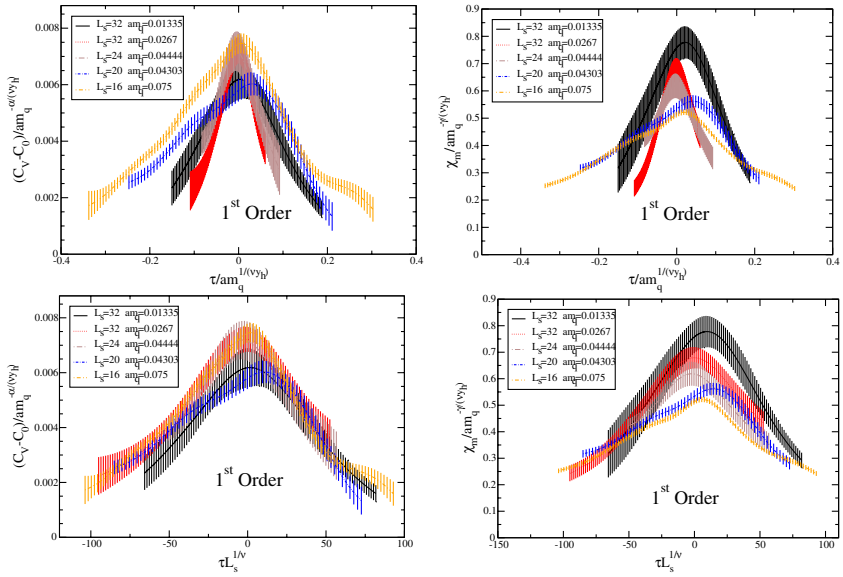

FIG. 9 (color online). Comparison of specific heat (top) and χ_m (bottom) scaling for first order. Equation (19) and (20).

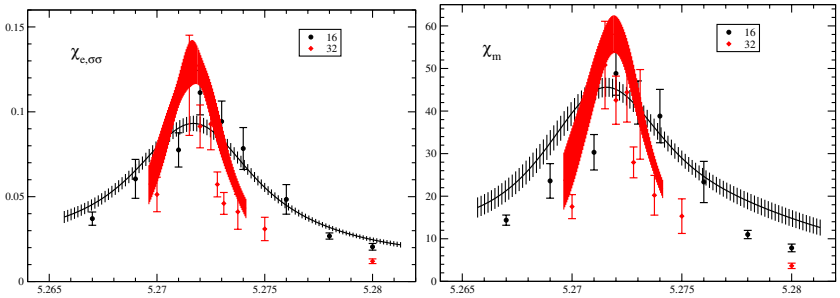

FIG. 10 (color online). Comparison between $\chi_{e,\sigma\sigma}$ (left) and χ_m (right) for $am_q = 0.013\,35$ and $L_s = 16, 32$.

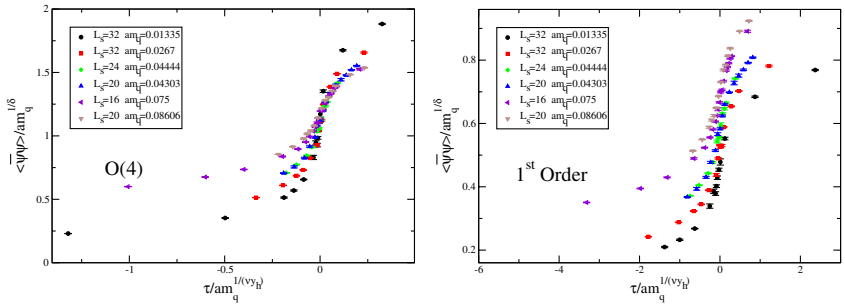

FIG. 11 (color online). Magnetic equation of state using nonsubtracted data for $O(4)$ (left) and first order (right).

critical part of the chiral condensate has to be zero far above the critical region. A tentative way to understand the noncritical background can be to assume it equal to the value $\langle\bar{\psi}\psi\rangle_\infty$ of $\langle\bar{\psi}\psi\rangle$ at $\beta = \infty$. This can be computed analytically and numerically on the flat configuration $U_{\mu\nu} = 1$. The result is

$$\langle\bar{\psi}\psi\rangle_\infty(am_q) = \frac{3}{L_s^3 L_t}\sum_{k_1,k_2,k_3,k_4} \times \frac{am_q}{(am_q)^2 + \sum_{i=1,2,3}(\sin\frac{\pi}{L_s k_i})^2 + (\sin\frac{\pi}{L_t(k_4+1/2)})^2} \tag{47}$$

which is almost a linear function in the mass range $am_q < 0.1$.

We then plot the subtracted value $\langle\bar{\psi}\psi\rangle_s \equiv \langle\bar{\psi}\psi\rangle - \langle\bar{\psi}\psi\rangle_\infty$ rescaled as $\langle\bar{\psi}\psi\rangle_s/(am_q)^{1/\delta}$ versus $\tau(am_q)^{-1/(\nu y_h)}$ to test the scaling Eq. (29). Figure 12 shows the result for $O(4)$ (similar figures being obtained with $O(2)$ and mean field). Visibly $O(4)$ scaling is not obeyed. An analogous investigation has been performed in Ref. [12], without the subtraction of the $\beta = \infty$ term: also in that case results were in disagreement with $O(4)$ scaling.

An alternative procedure is to subtract for each (am_q, L_s) the value at the largest measured β. The result is consistent with Fig. 12. A third possibility is to impose scaling at $\tau = 0$ and look if it is obeyed at $\tau \neq 0$. The result is shown in Fig. 13 and again there is no scaling.

As already explained in Section II, the analysis of Ref. [2] suggests to explore the possibility that the transition be a first order transition.

As a test of this possibility we have repeated the scaling analysis of the equation of state using first order critical indexes: the three procedures described above are consistent with each other and the result is shown in Fig. 14. A good scaling is observed.

We can investigate the consequence of the subtraction needed to isolate the critical part of $\langle\bar{\psi}\psi\rangle$ on the scaling of χ_m. If $\langle\bar{\psi}\psi\rangle - \langle\bar{\psi}\psi\rangle_\infty = am_q^{1/\delta}F(\tau/am_q^{1/\nu y_h})$ by differentiating with respect to am_q at fixed temperature we get

$$\chi_m - \frac{\partial}{\partial am_q}\langle\bar{\psi}\psi\rangle_\infty = \frac{1}{\delta}am_q^{1/\delta-1}F - \frac{1}{\nu y_h}am_q^{1/\delta-1}(\tau/am_q^{1/\nu y_h})F'. \tag{48}$$

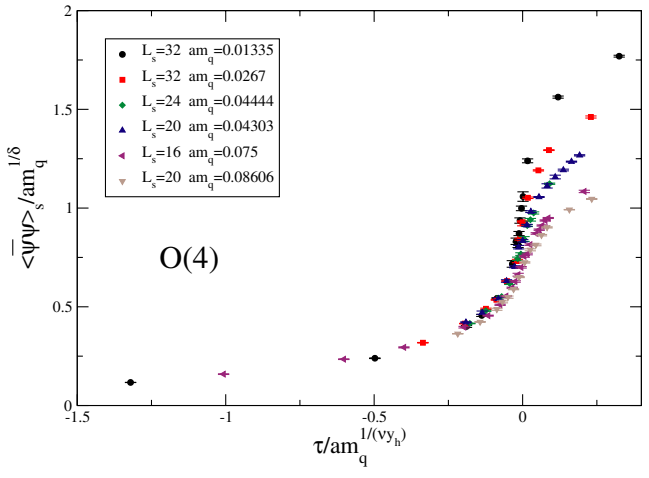

FIG. 12 (color online). Equation of state for $O(4)$, obtained by subtraction of $\langle\bar{\psi}\psi\rangle$ at $\beta = \infty$.

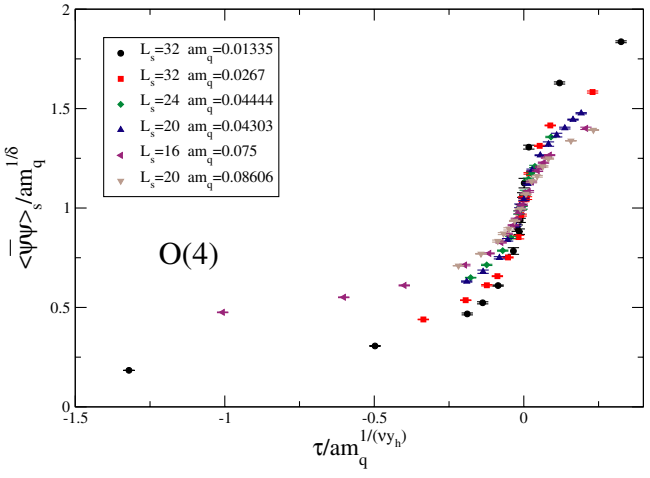

FIG. 13 (color online). Equation of state for $O(4)$, obtained by imposing scaling at $\tau = 0$.

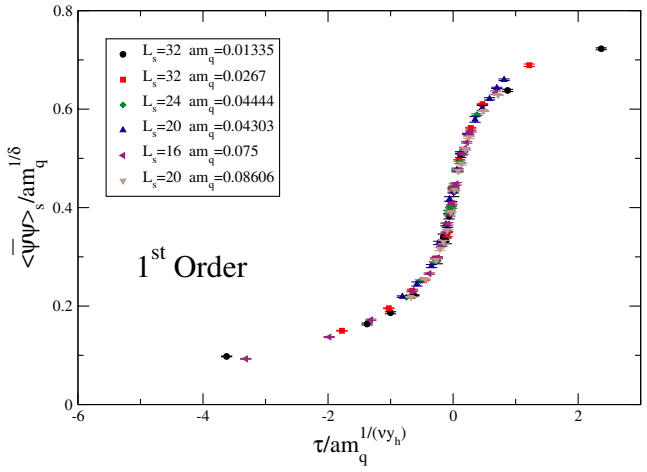

FIG. 14 (color online). Equation of state for first order.

Keeping in mind $1/\delta = (d - y_h)/y_h$, $\gamma = (2y_h - d)/y_t$ and $\nu = 1/y_t$ we find, at $\tau = 0$

$$am_q^{\gamma/\nu y_h}\left(\chi_m - \frac{\partial}{\partial am_q}\langle\bar{\psi}\psi\rangle_\infty\right) = \frac{1}{\delta}F(0). \qquad (49)$$

The quantity which scales is not $am_q^{\gamma/\nu y_h}\chi_m$ but a term $am_q^{\gamma/\nu y_h}\partial\langle\bar{\psi}\psi\rangle_\infty/\partial(am_q)$ must be added to it to get scaling. The subtraction of $\langle\bar{\psi}\psi\rangle$, due to the explicit breaking of chiral symmetry at $am_q \neq 0$, implies a subtraction for χ_m (which in the mass range of interest is almost constant).

This suggests to repeat the test of scaling for χ_m (Figs. 5–8) by introducing a subtraction by a constant to be determined. The content of Fig. 10 instead stays unchanged since the curves refer to the same value of the mass.

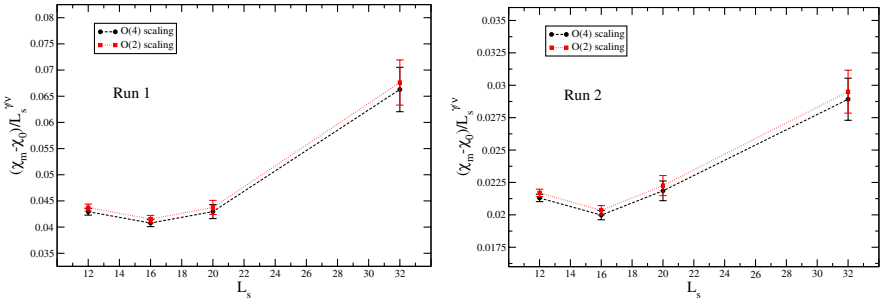

FIG. 15 (color online). Scaling of the maxima of $\chi_m - \chi_0$ at fixed $am_q L_s^{y_h}$ for Run1 (left) and Run2 (right). Two curves are shown corresponding to $O(4)$ (circles) and $O(2)$ (squares) critical behavior. The value of χ_0 is obtained by a best fit procedure.

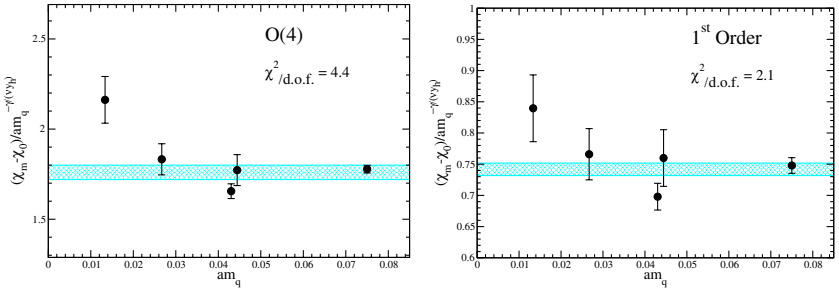

FIG. 16 (color online). Scaling of the maxima of $\chi_m - \chi_0$ at small am_q for $O(4)$ (left) and first order (right). The value of χ_0 is obtained by a best fit procedure. The χ^2/d.o.f. of the best fit is also shown.

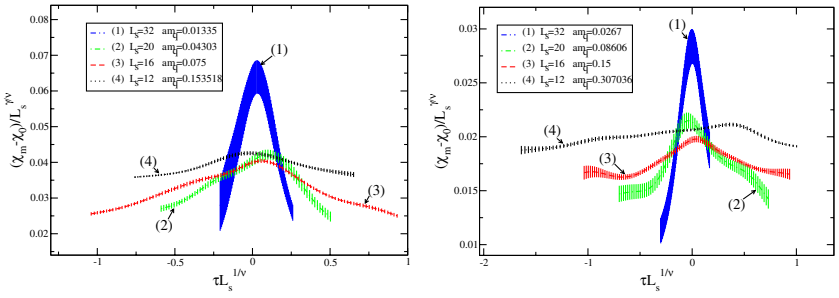

FIG. 17 (color online). Scaling of subtracted chiral condensate $\chi_m - \chi_0$ for Run1 (left) and Run2 (right). The background value χ_0 is obtained from a best fit of the peak value.

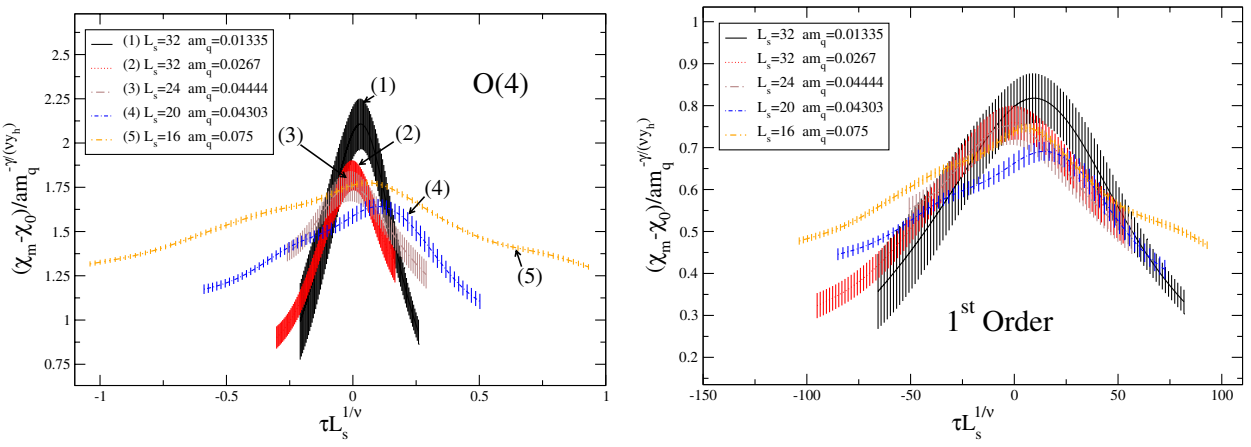

FIG. 18 (color online). Scaling of subtracted chiral condensate $\chi_m - \chi_0$ at small am_q for $O(4)$ (left) and first order (right). The background value χ_0 is obtained from a best fit of the peak value.

The best fit to determine the background is done by requesting scaling for the peaks of χ_m. The result is shown in Figs. 15 and 16. For $O(4)$—and $O(2)$—no scaling is obtained. A reasonable scaling results for first order. The corresponding modified scaling at all β's is shown in Figs. 17 and 18.

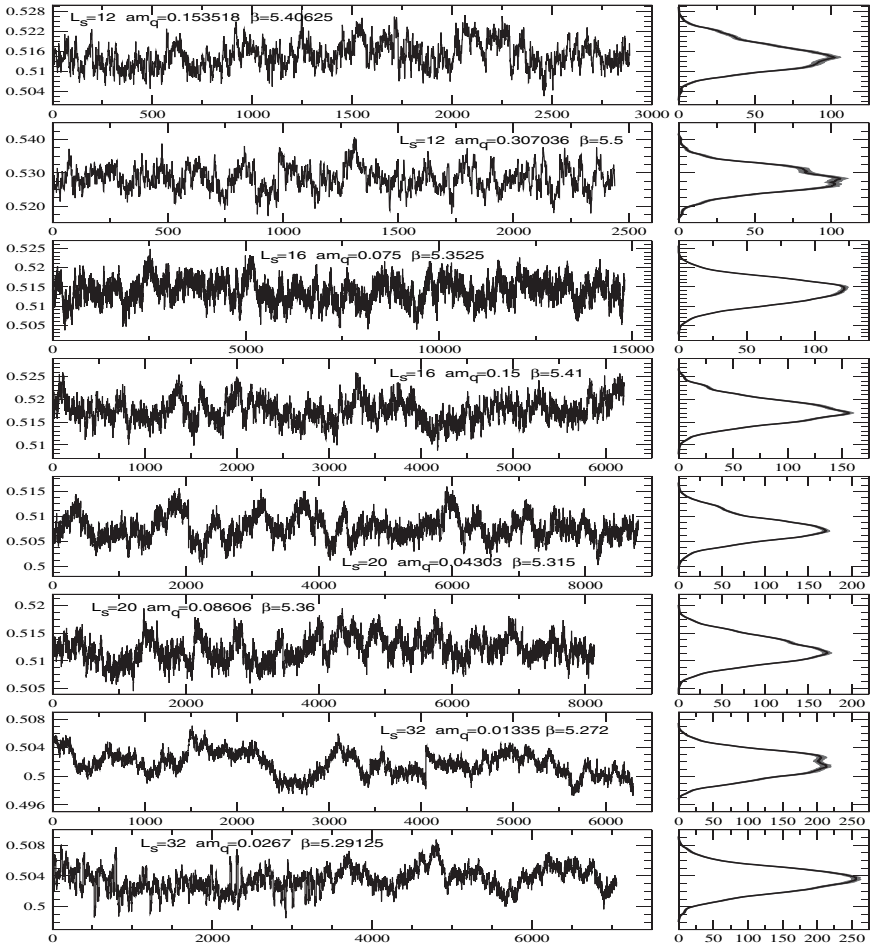

FIG. 19. Probability distribution function of average plaquette. Chiral condensate shows a similar behavior.

We notice that, due to the dependence of the temperature T on am_q and not only on β the definition of $\langle\bar{\psi}\psi\rangle = \frac{\partial \ln Z}{\partial m}|_T$ and $\chi_m = \frac{\partial^2 \ln Z}{\partial m^2}|_T$ must be revised, resulting in a combination of several terms analogous to what happens for the specific heat.

Analogously to what has been done for the specific heat, we have not refined consequently our analysis. Our investigation is exploratory: our L_t is not big enough, our action is not improved. We will extensively use the correct definitions in the planned improved version of this investigation.

E. Metastabilities

A first order chiral transition implies first order also at $m \neq 0$ and this should be visible in time histories. Metastable states should be present and should be visible as double peak structures in the histograms of distributions of the value of observables for large enough volumes. Although the results for scaling presented in the previous sections indicate that our volumes are not large enough, we have analyzed the probability distribution function of a number of observables, in particular, of the spatial plaquettes. The results are shown in Fig. 19. As in previous works [7,11] no convincing metastability appears.

To estimate the probability distribution function (PDF) from a given finite data set a nonzero width of the integration region should be chosen. We assume for the width a value given by 100th of the difference between the largest and smallest entry in our dataset. Errors are estimated using the bootstrap technique.

V. DISCUSSION AND CONCLUSIONS

The study of the nature of the chiral transition of $N_f = 2$ QCD is of fundamental importance: a second order phase transition would mean crossover at $m \neq 0$ and also at finite chemical potential, implying the presence of a tricritical point in the $T - \mu$ plane detectable by heavy ion experiments; a first order phase transition would drastically change this scenario. Moreover this is relevant to understanding what confined and deconfined really means in nature, i.e. if they are two different phases of matter corresponding to different realizations of some symmetry with an order parameter, or are connected by a crossover.

Previous studies on the subject did not come to a definite conclusion, also because of the huge computer power required. We have approached the problem by dedicating a big amount of computer power and by proposing a novel strategy for the scaling study around the chiral critical point. In particular we have developed a scaling study which assumes the critical indexes of the expected second order universality class ($O(4)$ or $O(2)$ according to the analysis of Ref. [2]) to reduce to a one scale problem without any further assumption. In this way we have been able to definitively rule out the possibility of $O(4)$ or $O(2)$ critical indexes, in the limits of validity of our techniques (standard staggered fermions, $L_t = 4$ and hybrid R algorithm) which need to be checked.

We have introduced the mass dependence of the reduced temperature τ (Eq. (23)), which was neglected in previous works.

To explore the alternative of a first order transition we should repeat the same analysis assuming the first order indexes. We plan to do that with improved action and larger lattices: that also will be a big numerical effort. With our present data we have instead made an analysis to test the scaling as done in previous papers, i.e. by assuming that $am_\pi L_s \gg 1$ (Eq. (15) and (16)). The am_q dependence of the pseudocritical β cannot discriminate between $O(4)$, $O(2)$, and first order. However the behavior of the peak of both the specific heat and of the chiral susceptibility definitely excludes $O(4)$ and $O(2)$, but are qualitatively consistent with first order (Fig. 7 and 16).

As for the shape of the critical peaks again $O(4)$ and $O(2)$ are definitely ruled out. The dependence of the width on L_s shows that the limit in which the Eqs. (15) and (16) are valid is not reached. Instead a scaling at L_s/ξ fixed agrees with first order, and again definitely excludes $O(4)$ and $O(2)$.

The magnetic equation of state is also nicely compatible with first order.

An additional improvement with respect to previous works is that the additive subtraction of the specific heat Eqs. (7), (15), and (19) has been determined from the wings of C_V as a function of β and am_q. Also $\langle\bar{\psi}\psi\rangle$ needs a subtraction at $am_q \neq 0$, where it is not an exact order parameter. We have also shown that this implies a subtraction for the chiral susceptibility at $am_q \neq 0$.

No clear signal of metastability is observed.

We recall that our analysis is made with $L_t = 4$ and unimproved action in the same way as previous analyses. No definite conclusion can be drawn on the order of the transition from any of these analyses. A check with improved algorithm and action and possibly larger L_t will be needed to assess this issue on a firm basis.

Within these limits our data are incompatible with an $O(4)$, $O(2)$ transition, and definitely prefer first order.

We are planning a similar analysis with improved action using the exact PHMC algorithm and $L_t = 6$. A consistency check will also be the study of the η' mass at the deconfining transition, in accordance with the analysis of [2], and we are also working at it.

ACKNOWLEDGMENTS

We acknowledge useful discussion with L. Del Debbio, C. DeTar, E. Laermann, B. Lucini, G. Paffuti, and P. Petreczky. We also acknowledge F. Karsch and A. Ukawa for relevant remarks on a draft of the manuscript.

APPENDIX A: MONTE CARLO PARAMETERS AND RAW DATA

In this appendix we report the details of our numerical results. Time histories of the observables are also available at request.

In the early stages of the computations some of the susceptibilities were not measured. Blank entries in the following tables refer to missing data.

In some previous report the data for the plaquette susceptibilities were defined with an extra factor of $1/4$. Below we have eliminated it in agreement with definition Eq. (32) to (36).

The connected component χ_m^{conn} has been measured only at the β value nearest to the critical coupling (except for the run with $L_s = 24$, $am_q = 0.044\,44$).

TABLE IV. Mean value of plaquettes, chiral condensate, and energy density from MC simulation. The number of thermalized trajectories is also shown together with the estimated autocorrelation time (for P_s and $\langle\bar{\psi}\psi\rangle$).

β	# Traj.	P_σ	P_τ	$\langle\psi\psi\rangle$	$\langle\psi D_0\psi\rangle$	$\tau_{\mathrm{int}}(P_\sigma)$	$\tau_{\mathrm{int}}(\langle\psi\psi\rangle)$
$L_t = 4$			$L_s = 12$		$am_q = 0.153\,518$		
5.3	1300	0.478 80(16)	0.478 93(16)	1.074 50(60)	···	7.7(2.4)	1.47(20)
5.325	1300	0.485 78(17)	0.486 01(17)	1.046 38(59)	···	7.3(2.2)	1.71(26)
5.35	1300	0.493 37(21)	0.493 63(20)	1.013 00(79)	···	10(3.7)	3.90(87)
5.375	2930	0.500 82(12)	0.501 30(13)	0.979 09(55)	0.721 33(24)	9.2(2.0)	3.71(53)
5.375	1250	0.501 47(15)	0.501 77(15)	0.976 83(56)	···	6.0(1.7)	1.91(31)
5.3875	2860	0.506 37(16)	0.506 89(16)	0.950 72(81)	0.726 57(24)	12(3.2)	6.4(1.2)
5.3875	1200	0.506 53(30)	0.507 11(32)	0.9497(20)	···	18(9.3)	15(6.9)
5.4	2920	0.511 29(16)	0.511 96(18)	0.9233(11)	0.731 40(25)	9.7(2.2)	8.3(1.8)
5.4	1200	0.510 41(27)	0.511 05(34)	0.9275(20)	···	13(5.9)	16(7.7)
5.40625	2890	0.514 94(30)	0.515 76(36)	0.8990(26)	0.735 94(34)	32(14)	33(14)
5.40625	600	0.514 64(37)	0.515 82(34)	0.8986(31)	···	14(8.9)	16(10)
5.4125	2890	0.517 62(50)	0.518 69(57)	0.8796(43)	0.740 62(55)	72(46)	77(51)
5.4125	1200	0.519 55(36)	0.521 00(49)	0.8635(37)	···	22(12)	36(25)
5.418 75	2900	0.522 00(36)	0.523 57(40)	0.8470(28)	0.748 66(41)	46(23)	42(20)
5.418 75	840	0.522 47(49)	0.524 09(53)	0.8468(37)	···	20(13)	28(17)
5.425	2970	0.525 08(18)	0.526 92(23)	0.8255(17)	0.754 32(29)	13(3.5)	19(6.3)
5.425	1200	0.525 76(35)	0.527 74(37)	0.8204(29)	···	19(9.8)	20(11)
5.43125	2910	0.528 02(19)	0.529 90(21)	0.8063(15)	0.758 39(24)	17(5.4)	16(5.2)
5.431 25	540	0.529 52(58)	0.531 51(70)	0.7917(61)	···	40(44)	66(90)
5.4375	1300	0.531 52(17)	0.533 81(16)	0.7782(11)	···	8.2(2.6)	8.6(2.8)
5.45	1300	0.534 75(20)	0.537 30(22)	0.7598(16)	···	10(3.9)	12(5.1)
5.475	1300	0.541 53(11)	0.544 11(13)	0.721 34(77)	···	4.4(1.0)	5.7(1.5)
5.5	1300	0.546 14(10)	0.549 17(11)	0.698 62(54)	···	4.7(1.1)	3.42(70)
5.525	1350	0.550 52(10)	0.553 40(11)	0.679 37(54)	···	4.19(95)	3.41(70)
5.55	1350	0.554 344(89)	0.557 310(76)	0.664 12(41)	···	3.13(62)	2.22(37)
5.575	1350	0.558 004(86)	0.560 962(80)	0.651 03(40)	···	3.03(60)	2.14(35)
5.6	1350	0.561 446(72)	0.564 575(86)	0.638 26(36)	···	2.32(41)	2.20(36)
$L_t = 4$			$L_s = 16$		$am_q = 0.075\,000$		
5.3	670	0.488 22(16)	0.488 59(20)	0.8911(34)	0.7461(19)	7.1(2.9)	11(6.3)
5.33	4840	0.499 282(83)	0.499 991(91)	0.8124(14)	0.753 03(77)	12(2.5)	24(7.2)
5.3325	3600	0.500 22(12)	0.501 06(13)	0.8051(18)	0.754 63(95)	18(5.2)	14(4.4)
5.335	4000	0.501 64(13)	0.502 52(14)	0.7903(18)	0.757 43(89)	19(5.3)	17(5.5)
5.3375	4000	0.503 21(12)	0.504 18(14)	0.7779(20)	0.758 25(81)	20(5.7)	35(13)
5.34	4000	0.504 25(22)	0.505 30(24)	0.7667(23)	0.760 50(84)	47(20)	48(21)
5.345	4000	0.507 78(20)	0.509 05(23)	0.7337(24)	0.765 76(81)	40(16)	47(21)
5.3475	4000	0.510 42(22)	0.512 03(26)	0.7059(24)	0.772 30(90)	40(16)	48(21)
5.35	7130	0.511 26(18)	0.512 91(21)	0.6990(26)	0.772 90(70)	40(12)	55(19)
5.3525	14 800	0.513 97(16)	0.515 85(19)	0.6664(22)	0.778 62(49)	69(19)	78(23)
5.355	4000	0.516 14(35)	0.518 26(41)	0.6446(42)	0.782 17(90)	85(50)	91(55)
5.3575	3800	0.517 76(19)	0.520 04(23)	0.6246(23)	0.786 42(86)	36(14)	43(18)
5.36	13 200	0.519 41(13)	0.521 84(14)	0.6061(17)	0.789 04(46)	52(13)	55(14)

TABLE IV. (*Continued*)

β	# Traj.	P_σ	P_τ	$\langle\psi\psi\rangle$	$\langle\psi D_0\psi\rangle$	$\tau_{\rm int}(P_\sigma)$	$\tau_{\rm int}(\langle\psi\psi\rangle)$
5.365	4000	0.521 81(12)	0.524 39(15)	0.5812(18)	0.792 46(79)	21(6.5)	30(10)
5.37	4000	0.524 29(10)	0.527 14(12)	0.5557(18)	0.798 49(75)	17(4.5)	24(8.7)
5.38	3100	0.527 678(78)	0.530 747(84)	0.5235(15)	0.802 05(84)	9.9(2.2)	13(4.3)
5.4	1200	0.532 769(91)	0.535 84(10)	0.4894(24)	0.8055(13)	5.1(1.3)	10(4.8)
5.45	1300	0.542 526(64)	0.545 907(62)	0.4296(15)	0.8120(11)	3.14(64)	8.7(3.8)
5.5	1300	0.550 574(49)	0.553 907(47)	0.3947(10)	0.815 46(98)	2.24(40)	8.6(3.7)
5.6	775	0.564 279(58)	0.567 819(47)	0.350 47(99)	0.8180(15)	2.36(55)	31(28)
$L_t = 4$			$L_s = 20$		$am_q = 0.043\,030$		
5.28	250	0.486 65(16)	0.487 35(25)	0.8082(16)	···	4.7(2.6)	5.4(2.7)
5.285	300	0.789 18(16)	0.489 84(14)	0.7916(13)	···	8.6(5.9)	3.0(1.2)
5.29	250	0.491 54(24)	0.491 89(25)	0.7695(23)	···	10(8.9)	7.9(5.2)
5.295	250	0.493 34(46)	0.494 18(54)	0.7510(48)	···	21(25)	17(17)
5.3	250	0.495 26(28)	0.496 16(27)	0.7276(56)	···	13(12)	22(23)
5.305	8640	0.498 846(93)	0.499 99(10)	0.6983(11)	0.770 44(10)	36(9.4)	31(7.7)
5.31	5366	0.502 11(15)	0.503 51(17)	0.6598(23)	0.775 87(15)	44(16)	48(18)
5.3125	2758	0.504 76(16)	0.506 49(18)	0.6238(25)	0.781 78(20)	27(11)	33(14)
5.315	8798	0.507 75(18)	0.509 75(21)	0.5830(30)	0.788 10(29)	69(24)	76(28)
5.3175	550	0.509 32(43)	0.511 42(41)	0.5661(45)	0.789 06(47)	42(46)	27(26)
5.32	6178	0.512 68(16)	0.515 16(18)	0.5144(26)	0.798 08(20)	43(14)	45(15)
5.325	200	0.515 13(27)	0.517 91(36)	0.4769(33)	···	18(22)	15(12)
5.33	300	0.518 94(17)	0.522 18(20)	0.4298(30)	···	7.8(5.1)	10(8.3)
5.34	350	0.522 39(26)	0.525 57(33)	0.3933(43)	···	19(17)	22(22)
5.35	400	0.524 922(98)	0.528 34(10)	0.3677(15)	···	4.3(1.8)	7.3(4.3)
$L_t = 4$			$L_s = 32$		$am_q = 0.013\,350$		
5.24	350	0.479 565(70)	0.480 086(81)	0.7687(18)	0.7631(10)	5.0(2.4)	3.4(1.6)
5.26	293	0.488 04(10)	0.489 01(10)	0.6841(22)	0.7719(11)	13(11)	3.4(1.7)
5.27	1434	0.496 42(25)	0.498 12(28)	0.5523(40)	0.788 50(48)	78(74)	68(62)
5.2715	2323	0.500 38(47)	0.502 52(52)	0.4783(98)	0.797 08(59)	190(220)	190(230)
5.272	6300	0.501 73(22)	0.504 05(25)	0.4539(47)	0.799 52(33)	144(87)	147(90)
5.2725	3790	0.503 01(25)	0.505 48(29)	0.4287(55)	0.802 68(34)	106(71)	104(70)
5.2728	3175	0.504 22(18)	0.506 85(21)	0.4019(42)	0.805 61(27)	90(60)	86(57)
5.2731	2605	0.505 72(17)	0.508 54(20)	0.3786(56)	0.808 52(31)	77(53)	103(76)
5.273 75	1060	0.505 11(34)	0.507 92(41)	0.3859(65)	0.808 29(42)	130(190)	100(130)
5.275	494	0.507 61(24)	0.510 59(27)	0.3389(68)	0.812 28(65)	40(47)	62(82)
5.28	335	0.511 175(49)	0.514 484(69)	0.2679(12)	0.818 64(63)	3.7(1.5)	8.1(5.0)
5.285	277	0.513 34(12)	0.516 80(15)	0.2325(21)	0.822 38(67)	14(13)	14(13)
5.29	290	0.514 85(13)	0.518 41(15)	0.2097(19)	0.822 67(54)	17(17)	13(12)
5.32	380	0.522 467(59)	0.526 117(77)	0.143 94(68)	0.828 35(42)	4.2(1.8)	9.9(6.6)
5.4	295	0.537 482(40)	0.541 084(38)	0.093 89(20)	0.829 98(44)	2.5(1.0)	3.5(1.9)
$L_t = 4$			$L_s = 12$		$am_q = 0.307\,036$		
5.3	850	0.468 98(13)	0.468 98(13)	1.246 37(48)	···	3.8(1.0)	0.94(13)
5.325	350	0.474 66(23)	0.474 42(23)	1.232 97(71)	···	3.0(1.2)	1.11(26)
5.35	350	0.481 29(26)	0.481 42(23)	1.216 96(78)	···	4.4(2.0)	1.39(37)
5.375	350	0.488 52(26)	0.488 57(31)	1.198 82(72)	···	5.2(2.5)	1.67(45)
5.3875	350	0.492 44(40)	0.492 55(43)	1.188 51(97)	···	9.3(6.2)	3.4(1.3)
5.4	350	0.495 71(29)	0.495 75(33)	1.181 02(72)	···	7.0(4.1)	1.45(37)
5.4125	350	0.498 45(43)	0.498 52(42)	1.173 34(68)	···	14(12)	0.91(19)
5.425	850	0.502 47(23)	0.502 49(24)	1.163 07(55)	···	8.6(3.5)	2.87(67)
5.4375	850	0.506 62(29)	0.506 82(29)	1.150 84(62)	···	15(8.3)	3.49(91)
5.45	800	0.510 59(16)	0.510 91(13)	1.140 39(55)	···	5.1(1.6)	2.09(45)
5.475	3540	0.519 22(18)	0.519 76(21)	1.111 76(58)	0.673 91(17)	16(4.7)	8.2(1.6)
5.475	750	0.519 06(26)	0.519 34(29)	1.112 20(79)	···	10(5.3)	5.1(1.6)
5.4875	3530	0.523 52(17)	0.523 94(17)	1.096 38(59)	0.676 98(20)	10(2.4)	6.4(1.1)

TABLE IV. (*Continued*)

β	# Traj.	P_σ	P_τ	$\langle\psi\psi\rangle$	$\langle\psi D_0\psi\rangle$	$\tau_{\rm int}(P_\sigma)$	$\tau_{\rm int}(\langle\psi\psi\rangle)$
5.4875	700	0.523 33(51)	0.523 63(57)	1.0998(25)	···	24(17)	26(19)
5.493 75	3390	0.526 52(17)	0.527 21(17)	1.085 30(60)	0.680 75(23)	13(3.5)	6.9(1.2)
5.5	2440	0.528 30(20)	0.529 16(21)	1.077 92(79)	0.682 99(28)	10(2.7)	7.1(1.5)
5.5	600	0.528 14(26)	0.529 02(28)	1.0775(12)	···	6.6(2.8)	9.8(4.4)
5.50625	3370	0.530 98(16)	0.531 92(19)	1.067 66(83)	0.686 86(30)	12(3.0)	10(2.2)
5.5125	3460	0.534 36(23)	0.535 73(28)	1.0530(11)	0.692 00(32)	24(8.5)	20(6.2)
5.5125	700	0.534 50(41)	0.535 82(54)	1.0522(21)	···	19(13)	24(17)
5.525	3550	0.538 94(18)	0.540 74(19)	1.032 37(56)	0.698 51(16)	23(7.9)	8.4(1.6)
5.525	700	0.540 25(23)	0.542 16(24)	1.027 66(80)	···	9.6(4.5)	5.6(1.8)
5.5375	3430	0.542 920(92)	0.544 869(97)	1.019 47(33)	0.702 73(16)	7.4(1.4)	3.41(44)
5.5375	700	0.543 69(16)	0.545 87(26)	1.013 00(74)	···	5.5(2.0)	5.8(1.9)
5.55	1010	0.546 35(17)	0.548 04(22)	1.006 77(57)	0.705 57(29)	8.6(3.2)	3.20(74)
5.55	700	0.546 22(17)	0.548 39(23)	1.007 61(65)	···	5.4(1.9)	4.2(1.2)
5.575	700	0.551 33(13)	0.553 65(16)	0.990 23(37)	···	4.2(1.3)	1.69(30)
5.6	800	0.555 811(97)	0.558 27(12)	0.976 84(36)	···	2.77(69)	1.73(31)
$L_t = 4$			$L_s = 16$		$am_q = 0.150\,000$		
5.3	2050	0.4793 69(57)	0.479 526(69)	1.0705(14)	0.7156(10)	3.83(68)	12(4.2)
5.36	16 640	0.4968 33(32)	0.497 128(34)	0.993 18(58)	0.721 74(33)	7.95(70)	12(1.7)
5.38	13 550	0.503 516(45)	0.503 963(47)	0.960 41(68)	0.724 96(37)	10(1.1)	15(2.4)
5.39	9000	0.507 338(76)	0.507 820(82)	0.939 11(92)	0.728 02(47)	19(3.7)	22(4.8)
5.4	10 000	0.511 931(89)	0.512 70(10)	0.911 45(87)	0.733 79(45)	26(5.6)	30(7.0)
5.405	8550	0.514 155(98)	0.515 08(10)	0.8973(10)	0.736 80(53)	26(5.9)	28(7.3)
5.41	6200	0.517 56(18)	0.518 75(20)	0.8711(16)	0.743 04(61)	49(17)	64(27)
5.415	8800	0.521 14(12)	0.522 65(14)	0.8458(11)	0.750 12(48)	38(10)	42(13)
5.42	12 300	0.523 68(11)	0.525 43(13)	0.826 91(95)	0.754 09(39)	40(9.4)	49(12)
5.425	14 800	0.526 255(80)	0.528 209(93)	0.808 12(78)	0.758 26(36)	31(5.7)	37(7.7)
5.43	9000	0.528 538(79)	0.530 666(88)	0.790 81(77)	0.762 13(39)	21(4.1)	25(5.4)
5.44	7300	0.532 536(72)	0.534 865(86)	0.765 18(94)	0.767 26(50)	16(3.2)	26(7.2)
5.46	7350	0.537 987(39)	0.540 635(40)	0.730 47(74)	0.773 95(45)	6.83(85)	15(3.4)
5.47	1200	0.540 548(88)	0.543 324(97)	0.7165(16)	0.778 42(93)	5.1(1.30	8.9(4.8)
5.48	1250	0.542 541(75)	0.545 410(79)	0.7047(16)	0.7778(10)	4.20(99)	11(5.4)
5.49	1200	0.544 427(63)	0.547 232(66)	0.6980(15)	0.780 19(95)	3.48(76)	12(5.5)
5.5	1300	0.546 411(75)	0.549 302(69)	0.6877(16)	0.781 93(90)	4.14(96)	9.0(4.7)
5.52	900	0.549 775(69)	0.552 711(78)	0.6736(14)	0.783 12(98)	3.08(75)	8.6(4.5)
$L_t = 4$			$L_s = 20$		$am_q = 0.086\,060$		
5.3	400	0.486 532(88)	0.486 94(10)	0.923 67(65)	···	4.4(1.8)	1.09(25)
5.32	350	0.492 52(12)	0.492 81(12)	0.891 10(68)	···	5.4(2.8)	1.73(54)
5.34	750	0.500 22(20)	0.500 92(20)	0.8372(17)	···	17(11)	16(9.5)
5.345	750	0.503 03(23)	0.503 94(23)	0.8135(21)	···	26(20)	23(16)
5.35	250	0.505 94(15)	0.506 99(17)	0.7839(25)	···	4.7(2.7)	11(9.3)
5.355	700	0.508 21(20)	0.509 33(26)	0.7689(30)	···	17(11)	35(31)
5.36	8140	0.512 08(17)	0.513 59(20)	0.7305(19)	0.768 15(25)	76(29)	77(29)
5.365	8565	0.516 35(12)	0.518 29(13)	0.6858(15)	0.777 47(19)	47(14)	56(18)
5.37	5574	0.519 93(12)	0.522 23(13)	0.6488(15)	0.783 32(15)	43(15)	52(20)
5.375	800	0.522 49(15)	0.524 86(17)	0.6248(34)	···	14(7.7)	54(60)
5.38	350	0.524 01(20)	0.526 40(30)	0.6104(30)	···	11(8.4)	20(19)
5.385	300	0.526 44(15)	0.529 18(22)	0.5879(30)	···	7.4(4.7)	15(15)
5.4	400	0.530 95(11)	0.534 10(10)	0.5493(11)	···	6.1(3.1)	8.3(5.2)
5.42	900	0.536 151(62)	0.539 203(52)	0.513 30(51)	···	4.0(1.1)	5.4(1.7)
$L_t = 4$			$L_s = 32$		$am_q = 0.026\,700$		
5.26	149	0.484 00(21)	0.484 64(20)	0.7814(24)	0.7605(10)	10(11)	7.2(5.9)
5.28	650	0.4920 92(63)	0.493 055(77)	0.7023(10)	0.768 43(57)	8.1(3.7)	4.8(1.7)
5.285	378	0.495 88(13)	0.497 16(14)	0.6539(14)	0.775 61(65)	15(13)	9.8(6.2)

TABLE IV. (*Continued*)

β	# Traj.	P_σ	P_τ	$\langle\psi\psi\rangle$	$\langle\psi D_0\psi\rangle$	$\tau_{\rm int}(P_\sigma)$	$\tau_{\rm int}(\langle\psi\psi\rangle)$
5.29	1200	0.500 50(12)	0.502 16(15)	0.5884(18)	0.784 89(37)	34(23)	32(21)
5.291 25	3960	0.503 98(18)	0.506 05(21)	0.5299(33)	0.793 14(34)	98(61)	98(62)
5.2925	3450	0.504 096(99)	0.506 16(11)	0.5301(16)	0.793 19(24)	24(8.2)	24(8.4)
5.2925	3118	0.504 26(36)	0.506 35(41)	0.5273(58)	0.793 34(42)	230(250)	210(220)
5.293 75	950	0.506 41(12)	0.508 80(15)	0.4896(22)	0.798 04(42)	15(7.9)	19(11)
5.295	345	0.509 41(18)	0.512 19(22)	0.4374(41)	0.805 98(68)	23(24)	45(68)
5.3	465	0.512 593(80)	0.515 578(86)	0.3892(13)	0.810 64(48)	8.8(5.0)	11(7.1)
5.305	235	0.515 550(85)	0.518 729(87)	0.3448(11)	0.815 85(54)	7.3(5.3)	6.8(4.9)
5.31	300	0.517 129(79)	0.520 44(10)	0.3232(16)	0.818 16(62)	5.9(3.4)	10(8.9)
5.32	265	0.520 284(41)	0.523 703(41)	0.287 89(81)	0.820 37(46)	2.6(1.1)	8.6(5.5)
5.34	285	0.525 526(40)	0.529 029(39)	0.242 20(75)	0.824 83(47)	2.36(90)	7.4(4.9)
$L_t = 4$			$L_s = 16$		$am_q = 0.013\,350$		
5.267	9600	0.492 25(24)	0.493 48(28)	0.6246(34)	0.779 48(55)	112(49)	66(22)
5.269	6350	0.495 64(48)	0.497 25(54)	0.5688(88)	0.785 65(66)	170(110)	152(94)
5.271	6500	0.499 97(47)	0.502 14(54)	0.4872(93)	0.795 38(71)	110(57)	112(59)
5.272	12 400	0.502 48(63)	0.504 89(72)	0.434(13)	0.801 79(71)	250(140)	240(140)
5.273	6800	0.501 88(69)	0.504 21(79)	0.449(13)	0.799 47(79)	190(130)	170(110)
5.274	9350	0.505 19(50)	0.507 95(58)	0.388(12)	0.806 78(64)	180(100)	200(120)
5.276	2700	0.507 18(46)	0.510 10(53)	0.343(11)	0.811 74(81)	67(42)	72(49)
5.278	4200	0.509 95(16)	0.513 18(19)	0.2863(42)	0.816 73(55)	27(8.8)	42(17)
5.28	4200	0.511 61(14)	0.514 96(15)	0.2562(31)	0.819 63(53)	30(10)	35(13)
$L_t = 4$			$L_s = 24$		$am_q = 0.044\,440$		
5.3	1310	0.495 37(14)	0.496 19(16)	0.7421(17)	0.763 63(20)	22(11)	20(10)
5.31	2200	0.502 13(20)	0.503 55(23)	0.6645(29)	0.775 83(24)	41(22)	42(23)
5.312	1990	0.503 68(24)	0.505 18(27)	0.6465(35)	0.778 25(24)	56(38)	57(38)
5.314	2620	0.504 95(17)	0.506 63(18)	0.6310(27)	0.780 66(26)	38(18)	42(21)
5.316	2520	0.507 50(38)	0.509 45(44)	0.5953(63)	0.786 34(49)	150(150)	160(170)
5.318	2600	0.510 24(22)	0.512 49(25)	0.5554(35)	0.792 30(30)	59(36)	63(39)
5.32	2260	0.511 28(29)	0.513 60(31)	0.5430(43)	0.794 02(31)	89(71)	92(75)
5.325	1470	0.515 99(17)	0.518 79(18)	0.4773(28)	0.803 38(18)	28(15)	30(17)
5.33	1420	0.518 75(10)	0.521 73(10)	0.4426(15)	0.808 29(15)	17(7.7)	20(9.5)
5.34	1000	0.522 071(90)	0.525 27(10)	0.4049(16)	0.812 35(17)	13(6.2)	26(16)
5.35	900	0.525 419(69)	0.528 794(74)	0.371 28(93)	0.816 52(17)	7.4(2.7)	11(4.9)

TABLE V. Raw data from MC simulation of susceptibilities entering the specific heat.

β	# Traj.	$\chi_{e,\sigma\sigma}$	$\chi_{e,\sigma\tau}$	$\chi_{e,\tau\tau}$	$\chi_{e,f}$	$\chi_{e,\sigma}$	$\chi_{e,\tau}$
$L_t = 4$			$L_s = 12$		$am_q = 0.153\,518$		
5.3	1300	0.0584(40)	0.0407(40)	0.0619(44)	···	···	···
5.325	1300	0.0570(38)	0.0375(35)	0.0559(38)	···	···	···
5.35	1300	0.0638(45)	0.0416(38)	0.0579(36)	···	···	···
5.375	2930	0.0598(27)	0.0426(28)	0.0625(32)	1.186(30)	0.0149(57)	0.0432(60)
5.375	1250	0.0530(36)	0.0321(31)	0.0510(34)	···	···	···
5.3875	2860	0.0746(43)	0.0588(44)	0.0817(46)	1.174(30)	0.0424(78)	0.0741(88)
5.3875	1200	0.0711(86)	0.0577(90)	0.0821(96)	···	···	···
5.4	2920	0.0877(52)	0.0732(58)	0.0962(61)	1.316(34)	0.086(10)	0.121(12)
5.4	1200	0.0785(78)	0.0626(95)	0.084(10)	···	···	···
5.406 25	2890	0.1094(83)	0.100(10)	0.129(12)	1.508(41)	0.160(19)	0.209(25)
5.406 25	600	0.067(10)	0.050(10)	0.0705(97)	···	···	···
5.4125	2890	0.134(13)	0.124(14)	0.155(16)	1.640(52)	0.213(31)	0.269(34)
5.4125	1200	0.0848(90)	0.069(10)	0.095(12)	···	···	···
5.418 75	2900	0.1128(85)	0.100(10)	0.125(11)	1.477(42)	0.155(21)	0.207(24)

TABLE V. (*Continued*)

β	# Traj.	$\chi_{e,\sigma\sigma}$	$\chi_{e,\sigma\tau}$	$\chi_{e,\tau\tau}$	$\chi_{e,f}$	$\chi_{e,\sigma}$	$\chi_{e,\tau}$
5.418 75	840	0.105(13)	0.090(13)	0.112(15)	···	···	···
5.425	2970	0.0926(55)	0.0812(63)	0.1089(73)	1.370(36)	0.126(13)	0.173(17)
5.425	1200	0.0824(92)	0.0654(94)	0.085(10)	···	···	···
5.431 25	2910	0.0811(49)	0.0662(49)	0.0899(56)	1.221(32)	0.0654(92)	0.078(10)
5.431 25	540	0.0614(75)	0.0483(96)	0.069(11)	···	···	···
5.4375	1300	0.0521(36)	0.0344(34)	0.0532(34)	···	···	···
5.45	1300	0.0579(44)	0.0420(48)	0.0622(61)	···	···	···
5.475	1300	0.0425(24)	0.0265(24)	0.0452(29)	···	···	···
5.5	1300	0.0391(21)	0.0227(18)	0.0393(22)	···	···	···
5.525	1350	0.0379(19)	0.0222(17)	0.0415(21)	···	···	···
5.55	1350	0.0338(16)	0.0172(13)	0.0327(15)	···	···	···
5.575	1350	0.0320(16)	0.0152(11)	0.0287(13)	···	···	···
5.6	1350	0.0300(14)	0.0159(11)	0.0328(14)	···	···	···
$L_t = 4$			$L_s = 16$		$am_q = 0.075\,000$		
5.3	670	0.0627(64)	0.0427(68)	0.0618(68)	2.09(47)	−0.027(64)	−0.019(84)
5.33	4840	0.0732(33)	0.0573(33)	0.0808(36)	2.03(20)	0.040(27)	0.070(26)
5.3325	3600	0.0835(51)	0.0678(55)	0.0911(60)	2.36(26)	0.051(31)	0.069(32)
5.335	4000	0.0939(53)	0.0784(57)	0.1042(62)	2.26(22)	0.122(42)	0.140(41)
5.3375	4000	0.0790(52)	0.0660(58)	0.0942(65)	1.82(20)	0.073(25)	0.104(24)
5.34	4000	0.114(10)	0.102(11)	0.130(11)	1.98(21)	0.166(43)	0.216(39)
5.345	4000	0.1090(82)	0.0980(96)	0.126(10)	1.82(19)	0.105(33)	0.137(35)
5.3475	4000	0.126(11)	0.120(13)	0.152(15)	2.26(22)	0.231(47)	0.273(47)
5.35	7130	0.1415(88)	0.135(10)	0.169(11)	2.40(18)	0.283(40)	0.363(43)
5.3525	14 800	0.1549(90)	0.150(10)	0.186(11)	2.40(13)	0.257(28)	0.335(35)
5.355	4000	0.152(14)	0.148(17)	0.182(19)	2.27(24)	0.263(57)	0.321(63)
5.3575	3800	0.1086(78)	0.1002(88)	0.129(10)	1.94(21)	0.182(40)	0.218(36)
5.36	13 200	0.1161(63)	0.1079(71)	0.1372(78)	1.93(10)	0.195(24)	0.243(27)
5.365	4000	0.0806(62)	0.0706(72)	0.0978(84)	1.74(16)	0.104(30)	0.156(32)
5.37	4000	0.0750(40)	0.0615(45)	0.0847(52)	1.58(15)	0.083(26)	0.123(31)
5.38	3100	0.0552(30)	0.0395(29)	0.0605(32)	1.45(22)	0.074(25)	0.110(29)
5.4	1200	0.0483(32)	0.0323(30)	0.0512(35)	1.43(29)	−0.053(47)	0.038(32)
5.45	1300	0.0395(21)	0.0213(17)	0.0374(18)	1.19(18)	−0.040(35)	0.036(32)
5.5	1300	0.0321(15)	0.0142(11)	0.0293(14)	0.81(21)	0.003(21)	0.039(23)
5.6	775	0.0264(18)	0.0125(14)	0.0285(14)	1.19(30)	−0.030(27)	−0.000(34)
$L_t = 4$			$L_s = 20$		$am_q = 0.043\,030$		
5.28	250	0.069(10)	0.057(16)	0.093(22)	···	···	···
5.285	300	0.0531(76)	0.0307(78)	0.0479(74)	···	···	···
5.29	250	0.071(11)	0.052(10)	0.073(11)	···	···	···
5.295	250	0.114(46)	0.100(39)	0.126(40)	···	···	···
5.3	250	0.073(13)	0.054(10)	0.075(10)	···	···	···
5.305	8640	0.1101(55)	0.0982(60)	0.1256(67)	3.311(50)	0.144(13)	0.1997(15)
5.31	5366	0.151(11)	0.146(12)	0.181(14)	3.383(66)	0.246(28)	0.316(30)
5.3125	2758	0.129(14)	0.166(16)	0.144(18)	3.056(87)	0.195(36)	0.252(44)
5.315	8798	0.195(17)	0.196(19)	0.239(22)	3.440(82)	0.390(44)	0.481(51)
5.3175	550	0.110(19)	0.096(20)	0.120(21)	2.50(20)	−0.017(63)	−0.020(70)
5.32	6178	0.177(13)	0.175(14)	0.213(16)	2.869(64)	0.316(34)	0.403(38)
5.325	200	0.0579(93)	0.041(14)	0.065(25)	···	···	···
5.33	300	0.0603(85)	0.0460(92)	0.067(12)	···	···	···
5.34	350	0.0724(88)	0.060(11)	0.080(13)	···	···	···
5.35	400	0.0444(57)	0.0262(49)	0.0462(48)	···	···	···
$L_t = 4$			$L_s = 32$		$am_q = 0.013\,350$		
5.24	350	0.0639(67)	0.0455(78)	0.0642(93)	10(1.4)	0.03(10)	0.133(81)
5.26	293	0.0551(78)	0.0394(73)	0.0628(77)	10(1.7)	0.06(10)	0.157(89)

TABLE V. (*Continued*)

β	# Traj.	$\chi_{e,\sigma\sigma}$	$\chi_{e,\sigma\tau}$	$\chi_{e,\tau\tau}$	$\chi_{e,f}$	$\chi_{e,\sigma}$	$\chi_{e,\tau}$
5.27	1434	0.205(40)	0.195(43)	0.226(47)	8.16(75)	0.38(11)	0.43(12)
5.2715	2323	0.46(11)	0.50(13)	0.59(14)	9.87(74)	0.70(27)	0.77(28)
5.272	6300	0.365(50)	0.394(54)	0.469(62)	8.59(36)	0.88(13)	1.04(15)
2.2725	3790	0.371(60)	0.398(68)	0.471(78)	8.17(43)	0.83(16)	0.97(19)
5.2728	3175	0.228(29)	0.231(32)	0.274(35)	6.23(32)	0.423(83)	0.498(92)
5.2731	2605	0.184(25)	0.184(31)	0.226(35)	6.50(37)	0.322(74)	0.435(87)
5.273 75	1060	0.164(41)	0.168(49)	0.212(57)	5.62(54)	0.34(16)	0.41(16)
5.275	494	0.123(27)	0.114(28)	0.145(31)	6.64(81)	0.234(97)	0.38(11)
5.28	335	0.0479(55)	0.0318(56)	0.0517(56)	3.95(68)	−0.002(53)	0.119(65)
5.285	277	0.0597(93)	0.050(10)	0.080(12)	3.79(59)	0.067(85)	0.085(68)
5.29	290	0.065(14)	0.055(14)	0.080(19)	2.22(34)	0.057(50)	0.093(77)
5.32	380	0.0567(50)	0.0369(58)	0.0591(71)	1.80(29)	−0.006(37)	0.019(35)
5.4	295	0.0389(38)	0.0199(28)	0.0351(29)	1.50(27)	−0.049(28)	0.015(29)
$L_t = 4$			$L_s = 12$		$am_q = 0.307\,036$		
5.3	850	0.0468(29)	0.0248(25)	0.0447(30)	···	···	···
5.325	350	0.0577(73)	0.0342(59)	0.0552(57)	···	···	···
5.35	350	0.0552(52)	0.0336(50)	0.0483(52)	···	···	···
5.375	350	0.0483(59)	0.0290(60)	0.0545(64)	···	···	···
5.3875	350	0.069(12)	0.049(11)	0.067(11)	···	···	···
5.4	350	0.0495(71)	0.0323(75)	0.058(10)	···	···	···
5.4125	350	0.0536(64)	0.0382(61)	0.0596(69)	···	···	···
5.425	850	0.0611(51)	0.0423(51)	0.0647(60)	···	···	···
5.4375	850	0.0626(68)	0.0419(68)	0.0606(73)	···	···	···
5.45	800	0.0422(29)	0.0259(27)	0.0453(29)	···	···	···
5.475	3540	0.0816(58)	0.0655(61)	0.0871(66)	0.791(19)	0.0633(90)	0.091(10)
5.475	750	0.0573(45)	0.0371(52)	0.0558(61)	···	···	···
5.4875	3530	0.0960(59)	0.0817(58)	0.1031(62)	0.830(21)	0.092(10)	0.121(10)
5.4875	700	0.084(10)	0.072(10)	0.094(12)	···	···	···
5.493 75	3390	0.0889(57)	0.0747(56)	0.0957(56)	0.845(21)	0.103(10)	0.128(11)
5.5	2440	0.0902(60)	0.0792(67)	0.1025(78)	0.883(26)	0.099(11)	0.137(13)
5.5	600	0.0652(65)	0.0482(73)	0.0655(76)	···	···	···
5.506 25	3370	0.0846(47)	0.0729(52)	0.0960(57)	0.895(24)	0.1103(93)	0.143(10)
5.5125	3460	0.0934(71)	0.0833(82)	0.1092(87)	0.877(26)	0.121(14)	0.159(15)
5.5125	700	0.0703(80)	0.0588(94)	0.0807(98)	···	···	···
5.525	3550	0.0693(46)	0.0546(48)	0.0729(50)	0.695(16)	0.0615(77)	0.0881(84)
5.525	700	0.0463(62)	0.0338(66)	0.0529(71)	···	···	···
5.5375	3430	0.0469(20)	0.0322(18)	0.0510(21)	0.611(14)	0.0227(35)	0.0475(37)
5.5375	700	0.0412(31)	0.0300(33)	0.0536(43)	···	···	···
5.55	1010	0.0451(33)	0.0324(37)	0.0568(51)	0.611(26)	0.0298(66)	0.0569(87)
5.55	700	0.0449(36)	0.0317(39)	0.0513(45)	···	···	···
5.575	700	0.0342(27)	0.0208(25)	0.0378(27)	···	···	···
5.6	800	0.0324(19)	0.0193(21)	0.0409(29)	···	···	···
$L_t = 4$			$L_s = 16$		$am_q = 0.150\,000$		
5.3	2050	0.0484(20)	0.0277(21)	0.0495(23)	1.47(22)	0.015(31)	0.049(23)
5.36	16 640	0.0610(12)	0.0421(11)	0.0620(12)	1.235(65)	0.019(10)	0.048(10)
5.38	13 550	0.0702(17)	0.0519(17)	0.0721(18)	1.260(73)	0.038(14)	0.065(13)
5.39	9000	0.0766(29)	0.0606(30)	0.0831(33)	1.345(91)	0.074(17)	0.090(19)
5.4	10 000	0.0860(34)	0.0722(38)	0.0969(43)	1.410(88)	0.072(16)	0.120(17)
5.405	8550	0.0887(37)	0.0738(38)	0.0964(41)	1.57(11)	0.098(19)	0.149(22)
5.41	6200	0.1156(86)	0.1066(97)	0.135(10)	1.52(13)	0.174(28)	0.215(35)
5.415	8800	0.1012(62)	0.0918(66)	0.1196(73)	1.332(98)	0.127(21)	0.187(23)
5.42	12 300	0.1043(51)	0.0958(60)	0.1250(69)	1.289(81)	0.152(16)	0.207(19)
5.425	14 800	0.0880(33)	0.0758(37)	0.1002(41)	1.314(72)	0.126(14)	0.171(16)
5.43	9000	0.0759(30)	0.0622(31)	0.0841(35)	1.205(81)	0.089(15)	0.120(17)

TABLE V. (*Continued*)

β	# Traj.	$\chi_{e,\sigma\sigma}$	$\chi_{e,\sigma\tau}$	$\chi_{e,\tau\tau}$	$\chi_{e,f}$	$\chi_{e,\sigma}$	$\chi_{e,\tau}$
5.44	7300	0.0663(28)	0.0523(31)	0.0739(35)	1.21(10)	0.065(16)	0.097(18)
5.46	7350	0.0470(13)	0.0313(12)	0.0498(13)	0.972(81)	0.033(13)	0.062(14)
5.47	1200	0.0440(27)	0.0285(24)	0.0463(28)	0.67(13)	0.046(29)	0.039(30)
5.48	1250	0.0409(23)	0.0266(22)	0.0449(27)	0.88(16)	0.001(34)	0.027(28)
5.49	1200	0.0355(19)	0.0200(17)	0.0391(20)	0.73(12)	0.030(34)	0.026(33)
5.5	1300	0.0426(23)	0.0261(20)	0.0441(22)	0.66(12)	−0.012(25)	0.016(24)
5.52	900	0.0334(21)	0.0157(17)	0.0324(22)	0.56(13)	−0.015(21)	0.002(22)
$L_t = 4$			$L_s = 20$		$am_q = 0.086\,060$		
5.3	400	0.0383(39)	0.0230(34)	0.0477(53)	⋯	⋯	⋯
5.32	350	0.0552(61)	0.0299(51)	0.0483(50)	⋯	⋯	⋯
5.34	750	0.086(11)	0.067(12)	0.085(12)	⋯	⋯	⋯
5.345	750	0.079(10)	0.063(11)	0.085(13)	⋯	⋯	⋯
5.35	250	0.0638(88)	0.0444(84)	0.0632(90)	⋯	⋯	⋯
5.355	700	0.078(12)	0.069(16)	0.096(18)	⋯	⋯	⋯
5.36	8140	0.166(12)	0.160(14)	0.194(15)	2.418(59)	0.047(27)	0.052(31)
5.365	8565	0.1316(82)	0.1235(94)	0.154(10)	1.943(50)	0.050(18)	0.056(21)
5.37	5574	0.1054(88)	0.0959(88)	0.1234(98)	1.670(40)	−0.013(14)	−0.012(16)
5.375	800	0.0667(83)	0.0506(89)	0.0710(91)	⋯	⋯	⋯
5.38	350	0.0696(98)	0.054(10)	0.081(14)	⋯	⋯	⋯
5.385	300	0.0490(73)	0.0396(86)	0.067(10)	⋯	⋯	⋯
5.4	400	0.0435(53)	0.0255(40)	0.0389(40)	⋯	⋯	⋯
5.42	900	0.0400(27)	0.0209(22)	0.0366(24)	⋯	⋯	⋯
$L_t = 4$			$L_s = 32$		$am_q = 0.026\,700$		
5.26	149	0.099(27)	0.076(25)	0.092(23)	5.6(1.2)	−0.11(14)	−0.10(13)
5.28	650	0.0643(59)	0.0472(75)	0.0706(87)	5.65(78)	0.039(55)	0.123(64)
5.285	378	0.081(23)	0.066(23)	0.090(26)	4.71(62)	0.034(77)	0.106(79)
5.29	1200	0.110(17)	0.100(18)	0.133(22)	4.35(37)	0.219(54)	0.286(51)
5.291 25	3960	0.253(40)	0.261(44)	0.312(50)	5.46(29)	0.58(12)	0.69(13)
5.2925	3450	0.286(21)	0.297(25)	0.351(28)	5.48(30)	0.589(65)	0.680(79)
5.2925	3118	0.303(92)	0.31(10)	0.37(12)	5.74(41)	0.65(26)	0.82(30)
5.293 75	950	0.176(34)	0.175(35)	0.215(39)	4.56(45)	0.35(11)	0.41(12)
5.295	345	0.102(19)	0.082(22)	0.100(25)	4.13(81)	0.127(73)	0.195(82)
5.3	465	0.0706(85)	0.0512(85)	0.0725(96)	3.44(36)	−0.031(53)	0.012(45)
5.305	235	0.0482(69)	0.0372(81)	0.0625(95)	2.16(36)	−0.030(48)	0.019(58)
5.31	300	0.0666(90)	0.0431(96)	0.0552(89)	3.02(51)	−0.024(50)	0.046(47)
5.32	265	0.0360(37)	0.0204(29)	0.0363(34)	2.04(32)	0.015(47)	0.036(47)
5.34	285	0.0364(33)	0.0163(27)	0.0355(30)	1.96(37)	−0.091(44)	0.029(38)
$L_t = 4$			$L_s = 16$		$am_q = 0.013\,350$		
5.267	9600	0.148(15)	0.141(17)	0.175(20)	9.75(31)	0.259(53)	0.327(64)
5.269	6350	0.242(45)	0.246(49)	0.294(56)	9.06(37)	0.41(11)	0.52(13)
5.271	6500	0.310(40)	0.323(43)	0.380(49)	7.81(35)	0.63(11)	0.72(13)
5.272	12 400	0.445(52)	0.478(60)	0.558(67)	8.40(29)	0.95(13)	1.13(14)
5.273	6800	0.377(48)	0.401(50)	0.470(56)	7.74(34)	0.75(12)	0.89(13)
5.274	9350	0.313(49)	0.328(59)	0.386(68)	7.16(31)	−0.111(90)	−0.13(10)
5.276	2700	0.193(34)	0.195(39)	0.235(44)	5.47(33)	0.301(72)	0.404(81)
5.278	4200	0.1073(73)	0.0958(87)	0.1236(97)	4.20(19)	0.114(26)	0.185(29)
5.28	4200	0.0819(78)	0.0669(82)	0.0904(87)	3.88(20)	0.089(27)	0.136(28)
$L_t = 4$			$L_s = 24$		$am_q = 0.044\,440$		
5.3	1310	0.108(13)	0.095(16)	0.124(18)	3.13(12)	0.138(26)	0.166(32)
5.31	2200	0.171(17)	0.164(19)	0.198(21)	3.46(11)	0.304(41)	0.374(46)
5.312	1990	0.174(22)	0.171(26)	0.211(29)	3.24(10)	0.306(55)	0.372(61)
5.314	2620	0.156(21)	0.150(23)	0.187(25)	3.35(11)	0.295(56)	0.379(63)
5.316	2520	0.187(39)	0.187(41)	0.230(49)	3.37(18)	0.38(12)	0.48(11)

TABLE V. (*Continued*)

β	# Traj.	$\chi_{e,\sigma\sigma}$	$\chi_{e,\sigma\tau}$	$\chi_{e,\tau\tau}$	$\chi_{e,f}$	$\chi_{e,\sigma}$	$\chi_{e,\tau}$
5.318	2600	0.170(18)	0.165(21)	0.199(24)	3.10(10)	0.333(49)	0.411(55)
5.32	2260	0.184(28)	0.183(32)	0.225(32)	2.97(11)	0.335(68)	0.409(65)
5.325	1470	0.128(19)	0.117(20)	0.143(21)	2.346(92)	0.189(45)	0.248(51)
5.33	1420	0.0760(75)	0.0595(81)	0.0824(82)	1.883(75)	0.043(14)	0.084(16)
5.34	1000	0.0579(74)	0.0419(78)	0.0615(86)	1.621(71)	0.038(12)	0.070(16)
5.35	900	0.0556(42)	0.0365(41)	0.0561(43)	1.456(68)	0.018(11)	0.060(12)

TABLE VI. Raw data from MC simulation for chiral condensate susceptibility and thermal susceptibility.

β	# Traj.	χ_m^{disc}	$\chi_{t,\sigma}$	$\chi_{t,\tau}$	$\chi_{t,f}$
$L_t = 4$		$L_s = 12$		$am_q = 0.153\,518$	
5.3	1300	0.859(32)	−0.183(21)	−0.204(21)	···
5.325	1300	0.806(31)	−0.180(20)	−0.173(18)	···
5.35	1300	0.863(37)	−0.238(23)	−0.227(22)	···
5.375	2930	0.947(27)	−0.238(15)	−0.241(17)	−0.077(42)
5.375	1250	0.726(27)	−0.167(16)	−0.157(15)	···
5.3875	2860	1.077(43)	−0.336(27)	−0.362(27)	−0.302(53)
5.3875	1200	1.17(11)	−0.353(62)	−0.397(69)	···
5.4	2920	1.396(67)	−0.468(35)	−0.510(43)	−0.639(81)
5.4	1200	1.117(91)	−0.368(54)	−0.402(64)	···
5.406 25	2890	1.95(17)	−0.730(77)	−0.810(95)	−1.37(18)
5.406 25	600	1.23(13)	−0.389(74)	−0.379(71)	···
5.4125	2890	2.31(22)	−0.91(10)	−1.00(12)	−1.81(23)
5.4125	1200	1.43(20)	−0.504(89)	−0.57(10)	···
5.418 75	2900	1.87(13)	−0.730(69)	−0.790(81)	−1.35(16)
5.418 75	840	1.51(17)	−0.62(11)	−0.67(12)	···
5.425	2970	1.585(97)	−0.588(45)	−0.669(52)	−1.09(12)
5.425	1200	1.34(14)	−0.497(73)	−0.535(75)	···
5.431 25	2910	1.316(75)	−0.296(31)	−0.324(35)	−0.697(81)
5.431 25	540	0.99(17)	−0.350(83)	−0.39(10)	···
5.4375	1300	0.709(42)	−0.230(23)	−0.245(23)	···
5.45	1300	0.859(67)	−0.291(32)	−0.324(38)	···
5.475	1300	0.486(30)	−0.157(15)	−0.178(17)	···
5.5	1300	0.384(16)	−0.1226(99)	−0.141(11)	···
5.525	1350	0.368(15)	−0.1287(90)	−0.1423(96)	···
5.55	1350	0.297(12)	−0.0956(76)	−0.1037(70)	···
5.575	1350	0.283(12)	−0.0885(74)	−0.0909(69)	···
5.6	1350	0.2442(92)	−0.0791(55)	−0.0944(61)	···
$L_t = 4$		$L_s = 16$		$am_q = 0.075\,000$	
5.3	670	1.61(34)	−0.25(13)	−0.30(17)	−0.82(61)
5.33	4840	1.82(21)	−0.381(58)	−0.425(60)	−0.20(27)
5.3325	3600	2.20(25)	−0.481(82)	−0.570(88)	−0.56(38)
5.335	4000	2.31(22)	−0.623(84)	−0.680(84)	−1.03(38)
5.3375	4000	2.79(32)	−0.619(85)	−0.596(76)	−1.20(34)
5.34	4000	3.89(37)	−1.09(12)	−1.24(13)	−1.77(39)
5.345	4000	4.05(37)	−1.11(12)	−1.14(12)	−1.81(43)
5.3475	4000	4.27(49)	−1.13(15)	−1.23(15)	−2.74(54)
5.35	7130	5.56(48)	−1.48(15)	−1.67(16)	−3.65(51)
5.3525	14 800	5.75(42)	−1.58(12)	−1.85(14)	−3.57(37)
5.355	4000	5.24(58)	−1.53(19)	−1.67(20)	−3.25(68)
5.3575	3800	3.74(39)	−0.99(12)	−1.07(12)	−2.26(43)
5.36	13 200	4.29(32)	−1.162(97)	−1.35(10)	−2.60(29)
5.365	4000	2.39(29)	−0.69(11)	−0.77(12)	−1.33(27)
5.37	4000	2.26(24)	−0.606(77)	−0.743(91)	−1.06(31)

TABLE VI. (*Continued*)

β	# Traj.	χ_m^{disc}	$\chi_{t,\sigma}$	$\chi_{t,\tau}$	$\chi_{t,f}$
5.38	3100	1.16(12)	−0.318(43)	−0.357(52)	−0.55(21)
5.4	1200	1.16(27)	−0.226(97)	−0.294(82)	0.00(35)
5.45	1300	0.501(95)	−0.116(40)	−0.184(43)	−0.09(24)
5.5	1300	0.233(73)	−0.065(31)	−0.098(40)	−0.02(10)
5.6	775	0.120(31)	−0.049(33)	−0.060(25)	0.17(13)
$L_t = 4$		$L_s = 20$		$am_q = 0.043\,030$	
5.28	250	3.16(35)	−0.43(11)	−0.64(17)	···
5.285	300	2.92(28)	−0.381(93)	−0.324(86)	···
5.29	250	3.60(40)	−0.56(12)	−0.53(12)	···
5.295	250	5.10(91)	−1.08(46)	−1.16(43)	···
5.3	250	5.4(1.1)	−0.66(18)	−0.70(16)	···
5.305	8640	5.27(24)	−1.109(72)	−1.227(80)	−2.25(17)
5.31	5366	7.57(61)	−1.75(16)	−1.96(19)	−3.95(41)
5.3125	2758	6.63(77)	−1.46(21)	−1.59(23)	−3.46(56)
5.315	8798	11(1.1)	−2.62(28)	−2.98(32)	−6.65(73)
5.3175	550	4.70(52)	−1.07(20)	−1.16(22)	0.38(80)
5.32	6178	10.26(89)	−2.37(21)	−2.67(24)	−5.55(55)
5.325	200	3.24(76)	−0.50(19)	−0.67(31)	···
5.33	300	3.02(60)	−0.58(13)	−0.65(18)	···
5.34	350	3.21(46)	−0.75(12)	−0.81(14)	···
5.35	400	1.39(17)	−0.293(64)	−0.325(60)	···
$L_t = 4$		$L_s = 32$		$am_q = 0.013\,350$	
5.24	350	9.3(1.3)	−0.53(18)	−0.40(20)	−1(2.2)
5.26	293	9.3(1.4)	−0.38(20)	−0.48(21)	−3(2.9)
5.27	1434	17(2.8)	−2.76(63)	−3.00(73)	−7(1.6)
5.2715	2323	50(10)	−6(2.3)	−7(2.6)	−23(5.0)
5.272	6300	42(5.6)	−7(1.0)	−8(1.1)	−19(2.9)
5.2725	3790	44(7.0)	−7(1.3)	−8(1.5)	−18(3.4)
5.2728	3175	27(3.6)	−4.45(67)	−4.92(71)	−9(1.8)
5.2731	2605	39(10)	−3.60(62)	−3.98(71)	−14(4.6)
5.273 75	1060	20(4.6)	−3.15(90)	−3(1.1)	−8(2.3)
5.275	494	15(4.0)	−2.10(81)	−2(1.0)	−6(1.9)
5.28	335	3.64(63)	−0.35(10)	−0.39(10)	−0.90(95)
5.285	277	5.65(93)	−0.77(21)	−1.02(28)	−2(1.4)
5.29	290	4.33(95)	−0.74(25)	−0.88(28)	−1.27(93)
5.32	380	1.15(13)	−0.284(48)	−0.332(52)	0.21(38)
5.4	295	0.083(14)	−0.046(14)	−0.042(15)	0.00(10)
$L_t = 4$		$L_s = 12$		$am_q = 0.307\,036$	
5.3	850	0.367(17)	−0.094(10)	−0.0813(96)	···
5.325	350	0.355(24)	−0.119(19)	−0.103(16)	···
5.35	350	0.373(28)	−0.092(17)	−0.097(18)	···
5.375	350	0.359(25)	−0.110(22)	−0.132(22)	···
5.3875	350	0.372(31)	−0.154(41)	−0.150(41)	···
5.4	350	0.367(26)	−0.115(25)	−0.103(28)	···
5.4125	350	0.320(21)	−0.089(18)	−0.090(18)	···
5.425	850	0.366(18)	−0.142(16)	−0.150(19)	···
5.4375	850	0.363(19)	−0.147(22)	−0.144(24)	···
5.45	800	0.350(18)	−0.094(12)	−0.110(12)	···
5.475	3540	0.591(21)	−0.250(22)	−0.270(25)	−0.147(34)
5.475	750	0.387(24)	−0.152(19)	−0.154(22)	···
5.4875	3530	0.674(23)	−0.322(26)	−0.347(26)	−0.327(41)
5.4875	700	0.594(75)	−0.305(51)	−0.334(54)	···
5.493 75	3390	0.654(24)	−0.302(26)	−0.328(25)	−0.362(40)
5.5	2440	0.675(31)	−0.333(28)	−0.364(32)	−0.377(48)

TABLE VI. (*Continued*)

β	# Traj.	χ_m^{disc}	$\chi_{t,\sigma}$	$\chi_{t,\tau}$	$\chi_{t,f}$
5.5	600	0.430(42)	−0.176(27)	−0.180(29)	···
5.506 25	3370	0.682(30)	−0.329(22)	−0.354(26)	−0.487(50)
5.5125	3460	0.727(42)	−0.366(33)	−0.409(37)	−0.552(74)
5.5125	700	0.488(45)	−0.254(35)	−0.284(44)	···
5.525	3550	0.513(17)	−0.234(19)	−0.246(21)	−0.185(29)
5.525	700	0.352(25)	−0.142(28)	−0.169(29)	···
5.5375	3430	0.399(10)	−0.1341(85)	−0.1474(86)	−0.001(17)
5.5375	700	0.317(18)	−0.108(12)	−0.148(17)	···
5.55	1010	0.337(16)	−0.126(12)	−0.146(17)	−0.094(31)
5.55	700	0.295(16)	−0.128(14)	−0.147(17)	···
5.575	700	0.221(10)	−0.0641(83)	−0.0866(83)	···
5.6	800	0.2125(99)	−0.0642(72)	−0.0863(89)	···
$L_t = 4$		$L_s = 16$		$am_q = 0.150\,000$	
5.3	2050	0.74(13)	−0.184(53)	−0.096(37)	0.28(25)
5.36	16 640	0.929(49)	−0.224(18)	−0.209(18)	−0.014(79)
5.38	13 550	1.062(69)	−0.320(27)	−0.317(27)	−0.21(10)
5.39	9000	1.296(95)	−0.412(40)	−0.442(40)	−0.25(15)
5.4	10 000	1.295(80)	−0.431(34)	−0.497(38)	−0.72(13)
5.405	8550	1.48(10)	−0.523(43)	−0.599(49)	−1.09(17)
5.41	6200	1.94(23)	−0.758(93)	−0.80(10)	−1.55(29)
5.415	8800	1.87(14)	−0.675(59)	−0.777(62)	−1.25(19)
5.42	12 300	1.88(11)	−0.672(50)	−0.793(53)	−1.18(14)
5.425	14 800	1.520(84)	−0.537(38)	−0.620(42)	−1.13(11)
5.43	9000	1.180(77)	−0.417(36)	−0.461(41)	−0.72(11)
5.44	7300	1.05(10)	−0.328(42)	−0.396(44)	−0.43(13)
5.46	7350	0.657(52)	−0.235(24)	−0.231(23)	−0.18(10)
5.47	1200	0.55(12)	−0.211(60)	−0.229(65)	−0.15(19)
5.48	1250	0.526(99)	−0.256(53)	−0.207(46)	0.02(23)
5.49	1200	0.49(10)	−0.194(59)	−0.171(54)	−0.18(21)
5.5	1300	0.54(10)	−0.180(48)	−0.195(48)	0.07(17)
5.52	900	0.283(70)	−0.100(30)	−0.106(44)	−0.06(11)
$L_t = 4$		$L_s = 20$		$am_q = 0.086\,060$	
5.3	400	1.384(93)	−0.145(28)	−0.184(37)	···
5.32	350	1.136(94)	−0.196(42)	−0.177(39)	···
5.34	750	2.04(29)	−0.56(11)	−0.58(11)	···
5.345	750	2.22(27)	−0.58(11)	−0.60(11)	···
5.35	250	2.31(27)	−0.49(11)	−0.521(98)	···
5.355	700	2.58(46)	−0.63(15)	−0.73(18)	···
5.36	8140	5.13(39)	−1.59(14)	−1.76(16)	−0.44(30)
5.365	8565	4.16(31)	−1.24(10)	−1.38(11)	−0.59(22)
5.37	5574	3.37(27)	−0.970(97)	−1.09(10)	0.07(19)
5.375	800	2.00(40)	−0.52(14)	−0.58(14)	···
5.38	350	1.77(32)	−0.46(13)	−0.58(14)	···
5.385	300	1.86(38)	−0.42(12)	−0.57(15)	···
5.4	400	0.810(98)	−0.243(39)	−0.227(36)	···
5.42	900	0.649(40)	−0.164(18)	−0.171(17)	···
$L_t = 4$		$L_s = 32$		$am_q = 0.026\,700$	
5.26	149	7.7(1.8)	−0.71(27)	−1.10(30)	0.6(2.4)
5.28	650	4.38(57)	−0.409(96)	−0.46(13)	−1.52(93)
5.285	378	5.9(1.0)	−0.76(33)	−0.80(32)	−1(1.3)
5.29	1200	6.98(84)	−1.21(24)	−1.44(27)	−3.71(79)
5.291 25	3960	18(3.0)	−4.01(70)	−4.43(77)	−10(2.1)
5.2925	3450	22(1.6)	−4.45(35)	−5.05(45)	−10(1.1)
5.2925	3118	23(6.9)	−4(1.6)	−5(1.8)	−11(4.3)

TABLE VI. (*Continued*)

β	# Traj.	$\chi_m^{\rm disc}$	$\chi_{t,\sigma}$	$\chi_{t,\tau}$	$\chi_{t,f}$
5.293 75	950	13(2.7)	−2.54(58)	−2.99(65)	−6(2.0)
5.295	345	5.9(1.2)	−1.13(24)	−1.26(30)	−3(1.2)
5.3	465	3.91(55)	−0.72(13)	−0.56(11)	−0.34(67)
5.305	235	2.28(42)	−0.46(11)	−0.42(11)	−0.80(63)
5.31	300	3.13(70)	−0.60(18)	−0.57(18)	−0.49(65)
5.32	265	1.55(25)	−0.236(85)	−0.304(80)	−0.64(50)
5.34	285	1.23(18)	−0.282(55)	−0.259(65)	−0.16(36)
$L_t = 4$		$L_s = 16$		$am_q = 0.013\,350$	
5.267	9600	14(1.1)	−2.08(29)	−2.30(36)	4.85(93)
5.269	6350	23(4.0)	−3.96(89)	−4(1.0)	−8(2.0)
5.271	6500	30(4.1)	−5.35(80)	−5.96(90)	−13(2.2)
5.272	12 400	48(5.1)	−8(1.0)	−9(1.1)	−20(2.5)
5.273	6800	42(5.0)	−7.19(98)	−8(1.0)	−17(2.6)
5.274	9350	38(6.2)	1.25(63)	1.44(72)	−16(3.3)
5.276	2700	23(4.8)	−3.84(84)	−4.30(95)	−8(1.6)
5.278	4200	11.00(97)	−1.64(18)	−1.90(20)	−3.57(60)
5.28	4200	7.84(90)	−1.15(17)	−1.27(18)	−2.51(58)
$L_t = 4$		$L_s = 24$		$am_q = 0.044\,440$	
5.3	1310	4.70(48)	−1.02(16)	−1.10(19)	−2.03(32)
5.31	2200	8.53(86)	−2.03(24)	−2.24(27)	−4.81(66)
5.312	1990	8.5(1.1)	−2.05(31)	−2.32(36)	−4.65(75)
5.314	2620	8.6(1.1)	−1.95(31)	−2.20(34)	−5.12(85)
5.316	2520	10(2.8)	−2.53(70)	−2.89(83)	−6(2.0)
5.318	2600	9.5(1.1)	−2.21(29)	−2.45(33)	−5.70(76)
5.32	2260	9.8(1.4)	−2.36(37)	−2.68(42)	−5.48(91)
5.325	1470	7.1(1.2)	−1.63(30)	−1.76(33)	−3.46(76)
5.33	1420	3.37(37)	−0.74(10)	−0.82(11)	−1.09(22)
5.34	1000	2.43(40)	−0.50(11)	−0.55(12)	−0.86(26)
5.35	900	1.56(14)	−0.365(50)	−0.412(50)	−0.70(11)

APPENDIX B: ESTIMATE OF THE BACKGROUND OF C_V

No significant dependence of the background C_0 from the volume of the system is expected since it is an ultraviolet quantity, while dependence on am_q and β is expected. In order to estimate $C_0(\beta, am_q)$ we performed a linear fit of the tails in the β region far from the peak for each different value of am_q. The procedure used is the following:

(a) first estimate the width W of the peak. The width that we choose to use as a reference is the width at 75% of the total height of the peak;

TABLE VII. Values of $\chi_m^{\rm conn}$ measured at the β nearest to the pseudocritical coupling. This value was taken as a constant through the critical region and added to $\chi_m^{\rm disc}$ to obtain χ_m.

L_s	am_q	β	# Traj.	$\chi_m^{\rm conn}$
12	0.153 518	5.4125	5600	1.01(5)
16	0.075	5.35	5000	1.59(10)
20	0.04303	5.315	2500	2.12(5)
32	0.01335	5.2725	120[a]	0.2(5)[a]
12	0.307 036	5.5	6200	0.55(3)
16	0.15	5.41	5000	1.00(5)
20	0.086 06	5.36	2550	1.3(1)
32	0.0267	5.2925	80[a]	0.4(2)[a]
24	0.044 44	5.316	3150	2.02(9)

[a]This quantity was measured only on a small fraction of configurations. Because of limited statistics the resulting value for $\chi_m^{\rm conn}$ is compatible with zero. However for these cases ($L_s = 32$ and $am_q = 0.013\,35, 0.0267$) $\chi_m^{\rm conn}$ is only a small fraction of χ_m and can be safely neglected within errors.

TABLE VIII. Pseudocritical couplings β_c estimated from the reweights curves for $\chi_{e,\sigma\sigma}$.

L_s	am_q	β_c
12	0.153 518	5.4112(18)
16	0.075	5.351 75(82)
20	0.043 03	5.3164(11)
32	0.013 35	5.271 80(20)
12	0.307 036	5.502(10)
16	0.15	5.411 53(61)
20	0.086 06	5.360 72(77)
32	0.0267	5.292 50(15)
24	0.044 44	5.3164(18)
16	0.013 35	5.271 68(27)

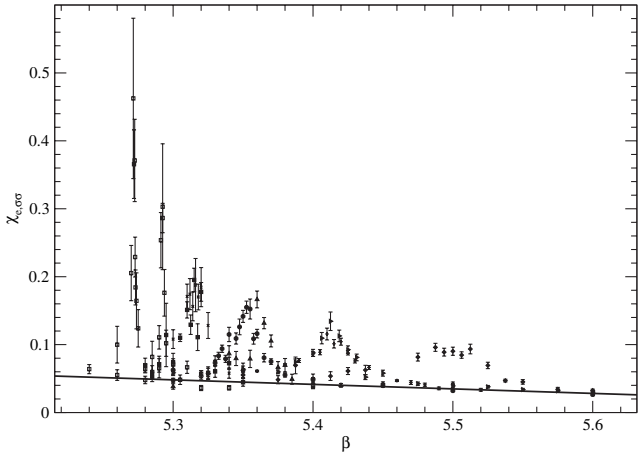

FIG. 20. Specific heat curves. The thick line shows the best linear fit for the background.

(b) then for each peak eliminate those points which lie in the β region around the maximum of the curve at distances smaller than $n \cdot W$, where n is a constant;
(c) fit the remaining points with a linear function and study the dependence of this fitted background on the parameter n.

For the whole procedure to make sense, we require that the background should fit better as n is increased. We require the value to be stable at sufficiently large n. This proves qualitatively to be the case. Since the number of points at large n is not large, we choose the best value of n by minimizing the reduced χ^2 of the fit of the background.

TABLE IX. $C_0(\beta)$ fit parameters for different values of n. The fit function is $C_0(\beta) = q_1 + q_2\beta$.

n	q_1	q_2	χ^2/d.o.f.	d.o.f.
3	0.608(60)	−0.103(11)	8.70	84
4	0.535(44)	−0.0908(84)	5.17	77
5	0.529(48)	−0.0887(88)	5.19	66
6	0.452(44)	−0.0751(80)	3.56	58
7	0.444(44)	−0.0740(80)	3.62	53
8	0.436(44)	−0.0728(80)	3.61	47
9	0.416(44)	−0.0693(77)	3.19	42
10	0.420(44)	−0.0695(75)	3.11	37
11	0.401(41)	−0.0661(77)	2.89	34
12	0.400(43)	−0.0663(83)	2.81	29
13	0.405(53)	−0.0668(97)	2.99	26
14	0.411(56)	−0.068(10)	2.95	24
15	0.404(56)	−0.067(10)	3.15	21

No dependence of the background on the bare quark mass am_q was found so we can take $C_0(\beta, am_q) = C_0(\beta)$. We choose then to do a global fit constraining all C_V peaks at different masses to share the same background. The result of this fit is shown in Fig. 20. The best fit is obtained excluding a region of width $12W$. Table IX shows the stability of the fit as the parameter n is in the range 6–15.

It should be noticed that even the β dependence is very weak and that $C_0(\beta)$ is consistent with a constant in the β range examined within the statistical errors so that the whole procedure described here is in practice equivalent to taking $C_0(\beta)$ a constant.

[1] A recent review on QCD thermodynamics is contained in: E. Laermann and O. Philipsen, Annu. Rev. Nucl. Part. Sci. **53**, 163 (2003).
[2] R. D. Pisarski and F. Wilczek, Phys. Rev. D **29**, 338 (1984).
[3] F. Wilczek, Int. J. Mod. Phys. A **7**, 3911 (1992).
[4] K. Rajagopal and F. Wilczek, Nucl. Phys. **B399**, 395 (1993).
[5] M. A. Stephanov, K. Rajagopal, and E. V. Shuryak, Phys. Rev. Lett. **81**, 4816 (1998).
[6] F. R. Brown, F. P. Butler, H. Chen, N. H. Christ, Z. Dong, W. Schaffer, L. I. Unger, and A. Vaccarino, Phys. Rev. Lett. **65**, 2491 (1990).
[7] M. Fukugita, H. Mino, M. Okawa, and A. Ukawa, Phys. Rev. Lett. **65**, 816 (1990).
[8] M. Fukugita, H. Mino, M. Okawa, and A. Ukawa, Phys. Rev. D **42**, 2936 (1990).
[9] F. Karsch, Phys. Rev. D **49**, 3791 (1994).
[10] F. Karsch and E. Laermann, Phys. Rev. D **50**, 6954 (1994).
[11] S. Aoki *et al.* (JLQCD Collaboration), Phys. Rev. D **57**, 3910 (1998).
[12] C. Bernard, C. DeTar, S. Gottlieb, U. M. Heller, J. Hetrick, K. Rummukainen, R. L. Sugar, and D. Toussaint, Phys. Rev. D **61**, 054503 (2000).
[13] A. A. Khan *et al.* (CP-PACS Collaboration), Phys. Rev. D **63**, 034502 (2001).
[14] M. D'Elia, A. Di Giacomo, and C. Pica, Nucl. Phys. B, Proc. Suppl. **140**, 541 (2005).
[15] M. E. Fisher and M. N. Barber, Phys. Rev. Lett. **28**, 1516 (1972).
[16] E. Brézin, J. Phys. (France) **43**, 15 (1982).
[17] T. Blum *et al.* (MILC Collaboration), Phys. Rev. D **51**, 5153 (1995).
[18] S. A. Gottlieb, W. Liu, D. Toussaint, R. L. Renken, and R. L. Sugar, Phys. Rev. D **35**, 2531 (1987).
[19] M. E. J. Newman and G. T. Barkema, *Monte Carlo Methods in Stastical Physics* (Oxford University, New York, 1999).
[20] F. Karsch, in Proceedings of the Workshop on Lattice Gauge Theory—A Challenge in Large Scale Computing, Wuppertal, Germany, 1985, Report. No. ILL-TH-86-9 (unpublished).